

# MicroRNA-195 在长期脑低灌注诱发认知功能障碍中的作用及其分子机制

张 帅 孙丽华 艾 静

哈尔滨医科大学药学院药理教研室, 哈尔滨, 150086, 中国



艾静,教授,哈尔滨医科大学药学院药理教研室,博士生导师。1991

年毕业于哈尔滨医科大学预防医学专业,2004年获得哈尔滨医科大学药理学博士学位,生物信息学和神经病理学博士后,龙江学者特聘教授,国务院和黑龙江省特殊津贴专家,哈尔滨医科大学教学名师。先后获得教育部新世纪优秀人才计划、黑龙江省杰出青年基金、第八届黑龙江省优秀青年科技奖、黑龙江省优秀教师、黑龙江省新长征突击手、黑龙江省师德建设十佳标兵和黑龙江省“五一”劳动奖章。现任中国药理学会神经药理专业委员会常务委员、抗衰老与老年痴呆专业委员会常务委员和分子生化药理专业委员会常务委员;中国老年学和老年医学学会老年病学分会认知障碍专家委员会委员、中国药理学会心血管药理专业委员会委员、黑龙江省医学会神经病学分会认知障碍学组副组长、《神经药理学报》编委。

自1999年开始从事药理学研究工作以来,荣获省部级以上科技进步奖8项。发表文章75篇,其中SCI论文50篇,被引用800余次。主编、副主编和参编人民卫生出版社“十二五”和“十三五”《药理学》规划教材和学习指导8部。

艾静教授先后从事抗心律失常药物和糖尿病药物的开发以及NPY在糖尿病性心脏病中的作用和机制的研究工作。2007年开始从事microRNAs在心源性猝死和更年期女性心脏疾病发生中的作用,并在国际上首次报导miR-1在心肌梗死患者血液中的表达变化可以成为预警心肌梗死的生物标记物、发现miR-23a以多靶点调控的方式通过调节心肌线粒体功能,参与更年期雌激素缺乏诱导的心肌重构和心律失常的过程,为未来miR-23a作为改善雌激素替代疗法或开发新药提供了实验依据;2009年开始从事microRNAs在老年痴呆发生和发展中的作用研究,并聚焦于探讨痴呆前期和早期的分子机制:发现在长期大脑低灌注的情况下,miR-195以多靶点调控的方式调节淀粉样多肽级联反应过程,在预防血管性痴呆发生中发挥重要作用;发现心脏过表达miR-1可以通过远端传输的机制影响认知功能相关蛋白的表达参与心脏疾病诱发认知功能损伤的过程。

该文重点回顾了,在长期大脑低灌注的情况下miR-195对大鼠认知功能的影响及其分子机制。

基金项目:国家自然科学基金资助项目(No. 81271207, 81471115, 81671052)

作者简介:张帅,男,硕士研究生;研究方向:神经药理学;E-mail:neurozhang\_s@163.com

通讯作者:艾静,女,教授,博士生导师;研究方向:神经药理学;Tel:+86-0451-86671354, Email: zhrbmu@126.com

**【摘要】**长期脑低灌注(chronic brain hypoperfusion, CBH)是血管性痴呆(vascular dementia, VD)患者共有的临床特征。探讨CBH对认知功能的影响对深入理解VD的发病机制,探索临床干预策略具有重要意义。课题组通过使用双侧颈总动脉结扎(bilateral common carotid artery occlusion, BCCAO,或two-vessel occlusion, 2VO)手术法构建CBH动物模型,并从miRNAs的角度系统研究了CBH对大鼠学习和记忆的影响及其分子机制。发现*microRNA-195*(*miR-195*)可以以多靶点调控的方式参与到老年痴呆的三个病理特征( $\beta$ 淀粉样蛋白(amyloid  $\beta$  peptide, A $\beta$ )沉积、tau蛋白过度磷酸化、神经元突触退化和神经元的死亡)的发生和发展过程中。值得关注的是,2VO引起的*miR-195*下调不仅可以通过上调淀粉样前体蛋白(amyloid precursor protein, APP)和 $\beta$ -分泌酶( $\beta$ -site APP cleaving enzyme 1, BACE1)的表达从源头启动A $\beta$ 级联反应过程,并且在这个级联反应过程的每一个关键节点处为维持反应过程提供底物。该系列研究也从另外一个角度证明miRNAs可以在一个功能模块中以多靶点调控的方式参与到疾病的发生和发展过程中。

**【关键词】**长期脑低灌注;痴呆;*miR-195*;淀粉样多肽级联反应

**【中国图书分类号】**R966      **【文献标志码】**A    **DOI:**10.3969/j.issn.2095-1396.2017.06.001

## The Action and Molecular Mechanisms of *MicroRNA-195* on Cognitive Decline Induced by Chronic Brain Hypoperfusion

ZHANG Shuai, SUN Li-hua, AI Jing

Department of Pharmacology, The State-Province Key Laboratories of Biomedicine-Pharmaceutics of China,  
College of Pharmacy of Harbin Medical University, Harbin, 150086, China

**【ABSTRACT】**Chronic brain hypoperfusion (CBH) is a common clinical manifestation of vascular dementia (VD). Clarifying the effects of CBH on cognitive function would help to improve our understanding the pathophysiological mechanism of VD and provide the possible therapeutic strategy for VD. In recent years, our group focused on to investigate the action and molecular mechanisms of CBH on learning and memory ability of rats using a CBH model by bilateral common carotid artery occlusion (or called two-vessel occlusion, 2VO). We found that *miR-195* could regulate cognitive ability of CBH rats through targeting on varies genes simultaneously that associated with all three pathological processes including amyloid  $\beta$  peptide (A $\beta$ ) deposition, tau hyperphosphorylation, dendritic degeneration and neuronal loss. Importantly, *miR-195* could not only prevent the initial amyloidogenic cascade response via downregulating amyloid precursor protein (APP) and  $\beta$ -site APP cleaving enzyme 1 (BACE1), but also provide sufficient requisite substrates during the amyloidogenic cascade response process. In addition, our series studies also provide evidence that miRNAs could participate in the onset and the development processes of diseases by regulating multi-targets within one functional module.

**【KEY WORDS】**chronic brain hypoperfusion; dementia; *microRNA-195*; amyloidogenic cascade response

长期脑低灌注(chronic brain hypoperfusion, CBH)是血管性痴呆(vascular dementia, VD)患者共有的临床特征<sup>[1]</sup>。临幊上轻度认知障碍(mild cognitive impairment, MCI)的患者往往伴有CBH,而MCI被认为是痴呆的临幊前阶段<sup>[1-2]</sup>。因此,CBH被认为可能是导致老年痴呆的重要因素之一。双侧颈总动脉结扎(bilateral common carotid artery occlusion, BCCAO,或two-vessel occlusion, 2VO)因可以产生明显的大脑低

灌注,被认为是目前公认的VD动物模型<sup>[3]</sup>。以往研究发现,CBH大鼠不仅表现为空间学习记忆能力下降,并且海马组织出现 $\beta$ 淀粉样蛋白(amyloid  $\beta$  peptide, A $\beta$ )沉积,但是确切的分子机制不清楚<sup>[4-5]</sup>。

自1993年报道了microRNAs(miRNAs)可以通过转录后调节蛋白的表达发挥生物学作用以来,miRNAs的研究就成为了生物医学研究的明星领域。miRNAs在老年痴呆中的作用研究也不例外。科学家

们已经发现多个 miRNAs 可以调节淀粉样前体蛋白 (amyloid precursor protein, APP) 和  $\beta$ - 分泌酶 ( $\beta$ -site APP cleaving enzyme 1, BACE1) 的表达, 参与 A $\beta$  的形成和聚集过程, 如 *miR-298*、*miR-328*、*miR-107*、*miR-29a/b-1*、*miR-9*、*miR-29c*、*miR-16*、*miR-17-5p*、*miR-20a*、*miR-101* 和 *miR-124* 等<sup>[6-10]</sup>。然而, 这些研究是在人或者动物的细胞系水平验证 miRNAs 和靶基因的调控关系, 或是观察 miRNAs 在阿尔茨海默病 (Alzheimer's disease, AD) 转基因小鼠脑组织中的表达。这些改变的 miRNAs 是继发于 AD 的结果还是导致 AD 的原因? 上述模型很难给予肯定的回答。此外, 作为具有多靶点调控功能的小分子 RNA, miRNAs 在 VD 众多的病理生理改变中是如何协调发挥作用的, 目前尚不清楚。因此, 本课题组通过采用 2VO 手术构建的 CBH 动物模型, 试图去寻找可能导致 VD 的分子机制, 为后续的药物研究提供理论依据。本文综述了近年来课题组在这一领域的研究结果。

### 1 *miR-195* 调节 CBH 引起的 A $\beta$ 聚集

在 A $\beta$  级联反应过程中, APP 在 BACE1 和  $\gamma$ - 分泌酶的作用下形成 A $\beta_{40}$  和 A $\beta_{42}$ , 其中 A $\beta_{42}$  容易产生折叠形成不溶性的聚集物, 即所谓的老年斑<sup>[11]</sup>。在这一过程中 BACE1 为限速酶。因此, 如果想要实现持续的 A $\beta$  的形成, 就需要有充足的代谢底物 APP 的生成和 BACE1 表达或活性的增强。课题组研究发现, 大鼠 2VO 手术 8 周后, 海马组织和血浆中 A $\beta_{40}$  和 A $\beta_{42}$  的水平均明显升高 (Fig.1), 同时海马和皮层 APP 和 BACE1 蛋白表达亦明显升高, 但 APP 和 BACE1 的 mRNA 表达基本不变 (Fig.2), 这一结果提示 2VO 引起的 APP 和 BACE1 蛋白表达变化存在转录后调控机制。通过检索 microRNAs 数据库 (Targets can 和 Pictar) 发现在 APP 和 BACE1 基因的 3'UTR 区均有 *miR-195* 的结合位点, 并且 qRT-PCR 检测证实 2VO 大鼠海马

和皮层 *miR-195* 表达均明显下降, 但其家族成员 *miR-16* 和 *miR-15b* 未发生改变 (Fig.3)。随后, 通过采用双萤光素酶报告基因、基因突变、*miR-195* 反义寡核苷酸 (AMO-195) 以及 miRNAs 屏障等技术证明 *miR-195* 可以通过与 APP 基因 3'UTR 区第 562-568 位点的核苷酸, 以及 BACE1 基因 3'UTR 区第 266-271 和 1795-1801 位点的核苷酸结合转录后调节 APP 和 BACE1 蛋白的表达 (Fig.4)<sup>[12]</sup>。为了验证 *miR-195* 是否可以在体内行使功能, 给 2VO 大鼠海马局部注射慢病毒携带的 *miR-195* 拟似物 (lenti-pre-*miR-195*), 发现 lenti-pre-*miR-195* 可以明显缓解 2VO 手术引起的大鼠空间学习和记忆能力的下降, 抑制 2VO 大鼠海马和皮层的 APP 和 BACE1 蛋白表达以及 A $\beta$  的生成 (Fig.5)。那么, 2VO 导致 *miR-195* 下降的机制又如何? 本课题组首先使用生物信息学技术进行预测发现核因子- $\kappa$ B (nuclear factor- $\kappa$ B, NF- $\kappa$ B) 在 *miR-195* 启动子区有 7 个结合位点, 通过采用免疫共沉淀技术进行筛查, 证明 NF- $\kappa$ B 与 *miR-195* 启动子区 -642~441 核苷酸之间有结合能力, 并有效抑制 *miR-195* 的表达 (Fig.6)<sup>[12]</sup>。

通过上述研究, 得出结论: 通过 2VO 手术构建的 CBH 模型可以诱导大鼠产生空间学习和记忆能力下降。其分子机制为 CBH 促进 NF- $\kappa$ B 的表达, NF- $\kappa$ B 抑制 *miR-195* 的表达, 下调的 *miR-195* 转录后调节 APP 和 BACE1 的表达, 使 APP 和 BACE1 表达上调, 导致 A $\beta$  沉积<sup>[12]</sup>。

### 2 *miR-195* 调节 CBH 引起的 tau 蛋白过度磷酸化

临床研究发现, 痴呆患者 tau 蛋白的磷酸化水平与痴呆严重程度成正相关<sup>[13]</sup>。那么, 2VO 是否也会促进 tau 蛋白的磷酸化过程, 其与 2VO 导致的 A $\beta$  沉积是否相关? 目前尚不清楚。本课题组的研究发现, 2VO 大鼠海马组织 tau 蛋白多个位点发生过度磷酸化的现象 (Fig.7)。有研究报道, A $\beta$  可以在 Ca<sup>2+</sup> 的协助下激活

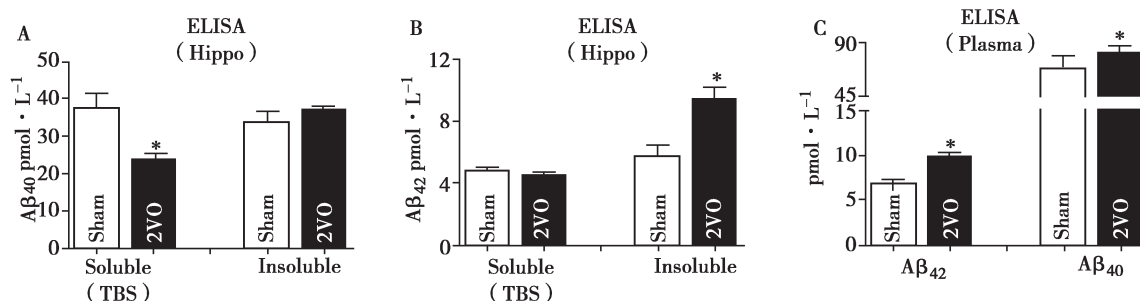


Fig. 1 Alterations of A $\beta$  levels in 2VO rats compared with sham-operated rats<sup>[12]</sup>

A, B: Soluble and insoluble A $\beta_{40}$  A and A $\beta_{42}$  B levels in hippocampi of 2VO rats and sham rats by ELISA assay. C: A $\beta_{42}$  and A $\beta_{40}$  levels in plasma of rats by ELISA assay. \*P<0.05 vs Sham,  $\bar{x} \pm s$ , n=5.

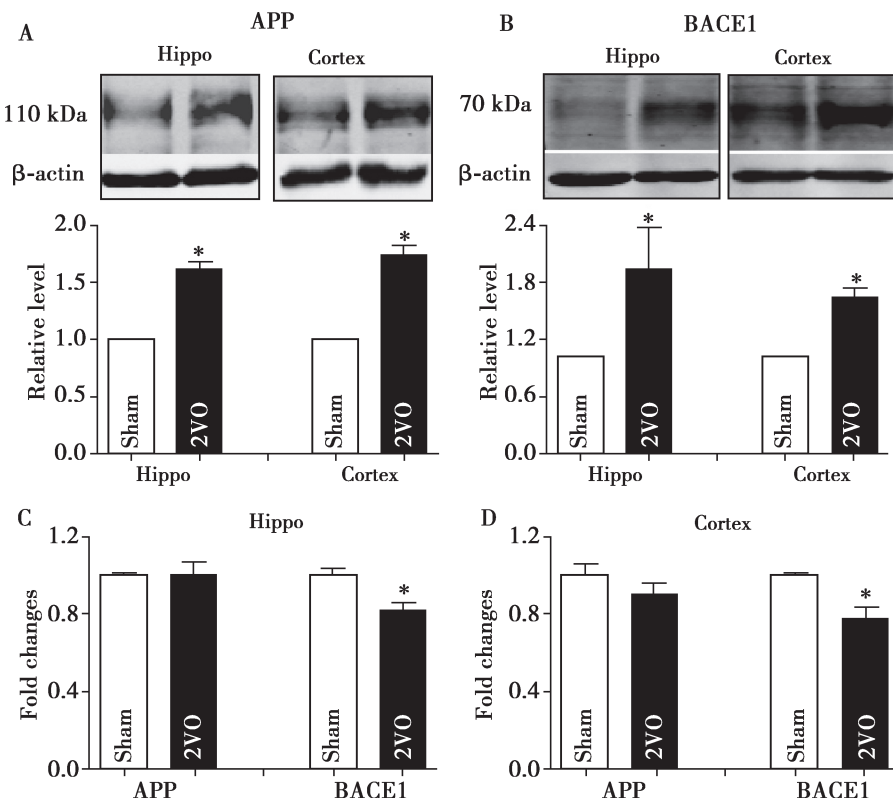


Fig. 2 Alterations of APP and BACE1 levels in 2VO rats compared with sham-operated rats<sup>[12]</sup>

A, B: Western blot analysis of hippocampi and cortices sham and 2VO rats, upper: representative immunoblots of APP, BACE1, and β-actin; lower: the quantitative analysis data of the immunoblots. C, D: The relative quantification of APP and BACE1 mRNA levels in hippocampi and cortices by real-time PCR. \*P<0.05 vs Sham,  $\bar{x} \pm s$ , n=7.

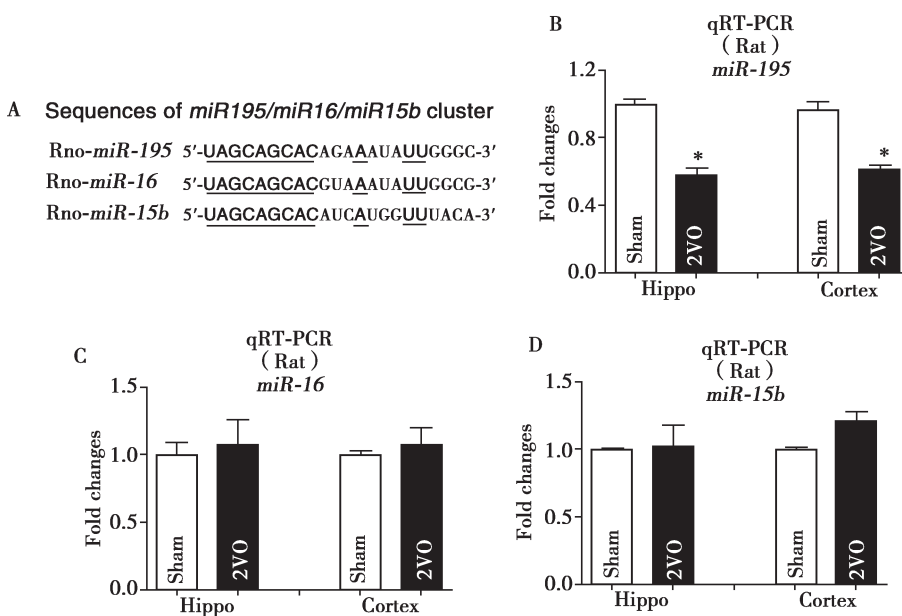


Fig. 3 Reduction of miR-195 level in 2VO<sup>[12]</sup>

A: Sequences for the miR-195/15b/16 family members. The conserved seed sequences among three microRNAs were marked by a square. B: MiR-195 levels as measured by qRT-PCR. C, D: No significant differences of miR-16 and miR-15b levels in hippocampi and cortices between 2VO and sham rats. \*P<0.05 vs Sham,  $\bar{x} \pm s$ , n=12.

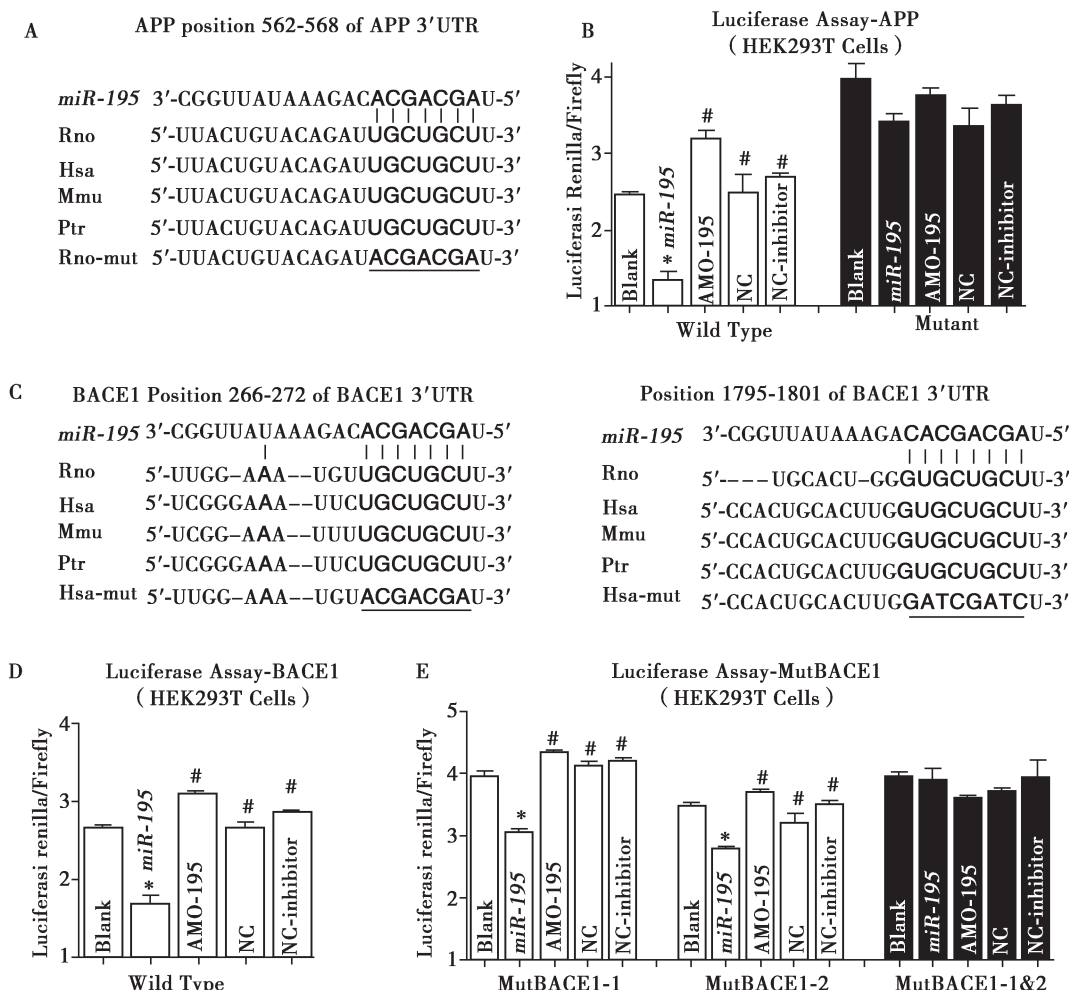


Fig. 4 APP and BACE1 are potential targets of miR-195<sup>[12]</sup>

A: Complementarity between *miR-195* seed sequence (5'end 2-8 nucleotides) and the 3'UTRs of rat's APP predicted by a computational and bioinformatics-based approach using the Targetscan algorithm. Watson-Crick complementarity is connected by “|”. The mutations made to the genes are indicated in red. B: Luciferase reporter gene assay for interactions between *miR-195* and its binding sites in the 3'UTRs of the APP mRNA in HEK293T cells. C: *miR-195* seed sequence (5'end 2-8 nucleotides) complementary with the 3'UTRs of rat's BACE1 predicted by a computational and bioinformatics-based approach using the Targetscan algorithm. Watson-Crick complementarity is connected by “|”. The mutations made to the genes are indicated in red. D, E: Luciferase reporter gene assay for interactions between *miR-195* and its binding sites D or mutation of binding site E in the 3'UTRs of the BACE1 mRNAs in HEK293T cells. \*P<0.05 vs NC, #P<0.05 vs *miR-195*,  $\bar{x} \pm s$ .

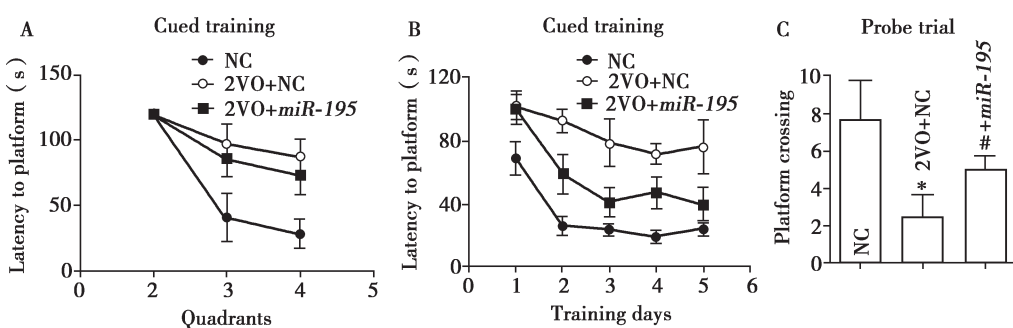


Fig. 5 *MiR-195* attenuates learning and memory deficits in 2VO model<sup>[12]</sup>

A: Comparison of average escape latency to find the platform from three non-target quadrants at training day 1 after 2VO and 2VO+lenti-pre-*miR-195* treatment for 8 weeks. B: Mean daily latencies to escape from the start point onto the hidden platform after 2VO and lenti-pre-*miR-195* treatment for 8 weeks. C: Number of times crossed the target platform location during probe trial.

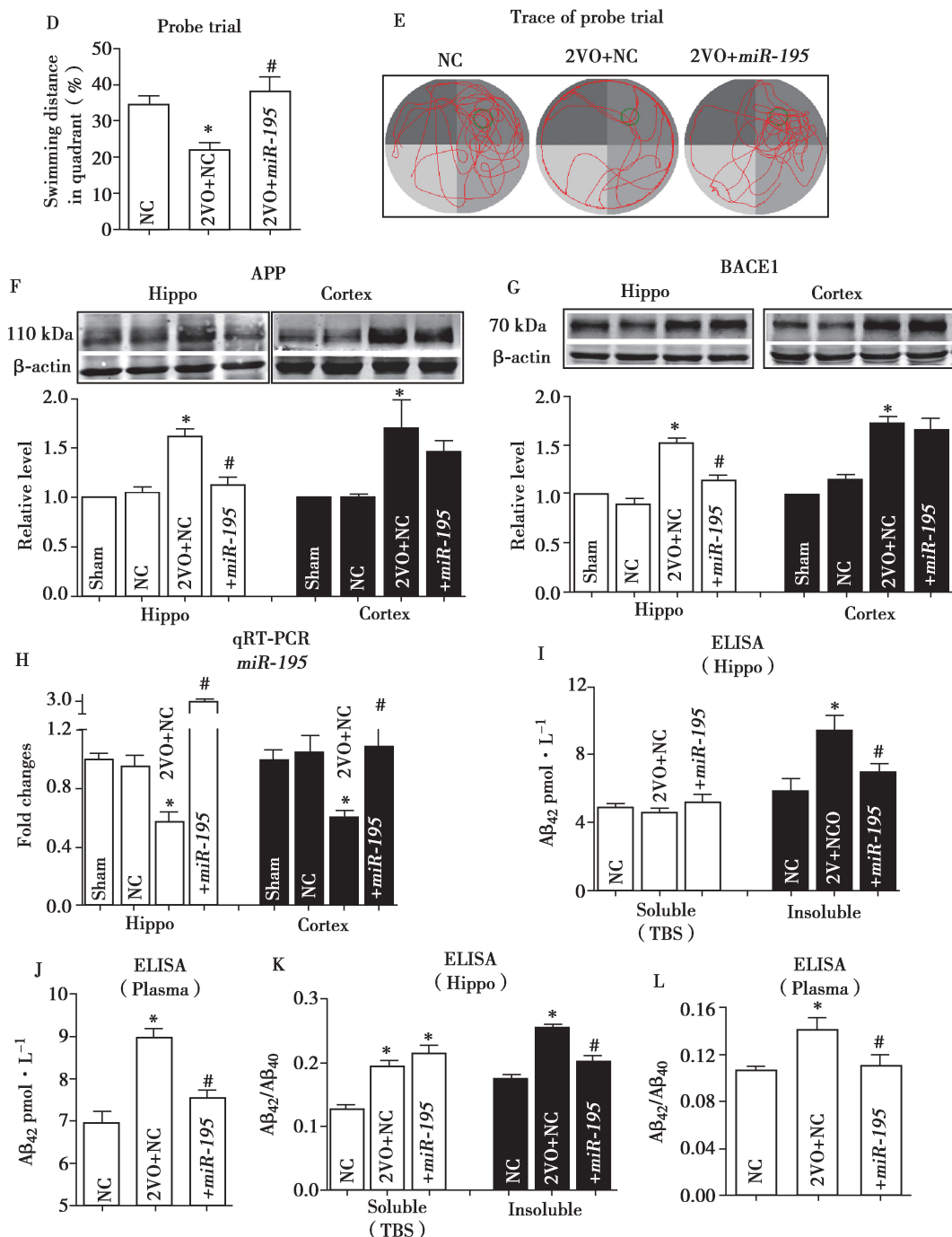


Fig. 5 (continued)

D: Swim distance in the target quadrant during probe trial. E: Representative path tracings of the probe test on day 6 in the MWM test for each group. Edge-type swim tracing was recorded in 2VO rats, which was reversed by lenti-pre-*miR-195*. F, G: APP F and BACE1 G protein expression in hippocampus and cortex in 2VO with or without lenti-pre-*miR-195* treatment for 8 weeks. H: Detection of *miR-195* in hippocampus and cortex of 2VO rats with or without lenti-pre-*miR-195* treatment. I: Aβ<sub>42</sub> levels in hippocampus from 2VO rats with or without lenti-pre-*miR-195* treatment and sham rats by ELISA assay. J: Aβ<sub>42</sub> levels in plasma by ELISA assay. K, L: The ratios of Aβ<sub>42</sub> / Aβ<sub>40</sub> in hippocampus tissues K and plasma L were compared. \*P<0.05 vs Sham, #P<0.05 vs 2VO,  $\bar{x} \pm s$ , n=5.

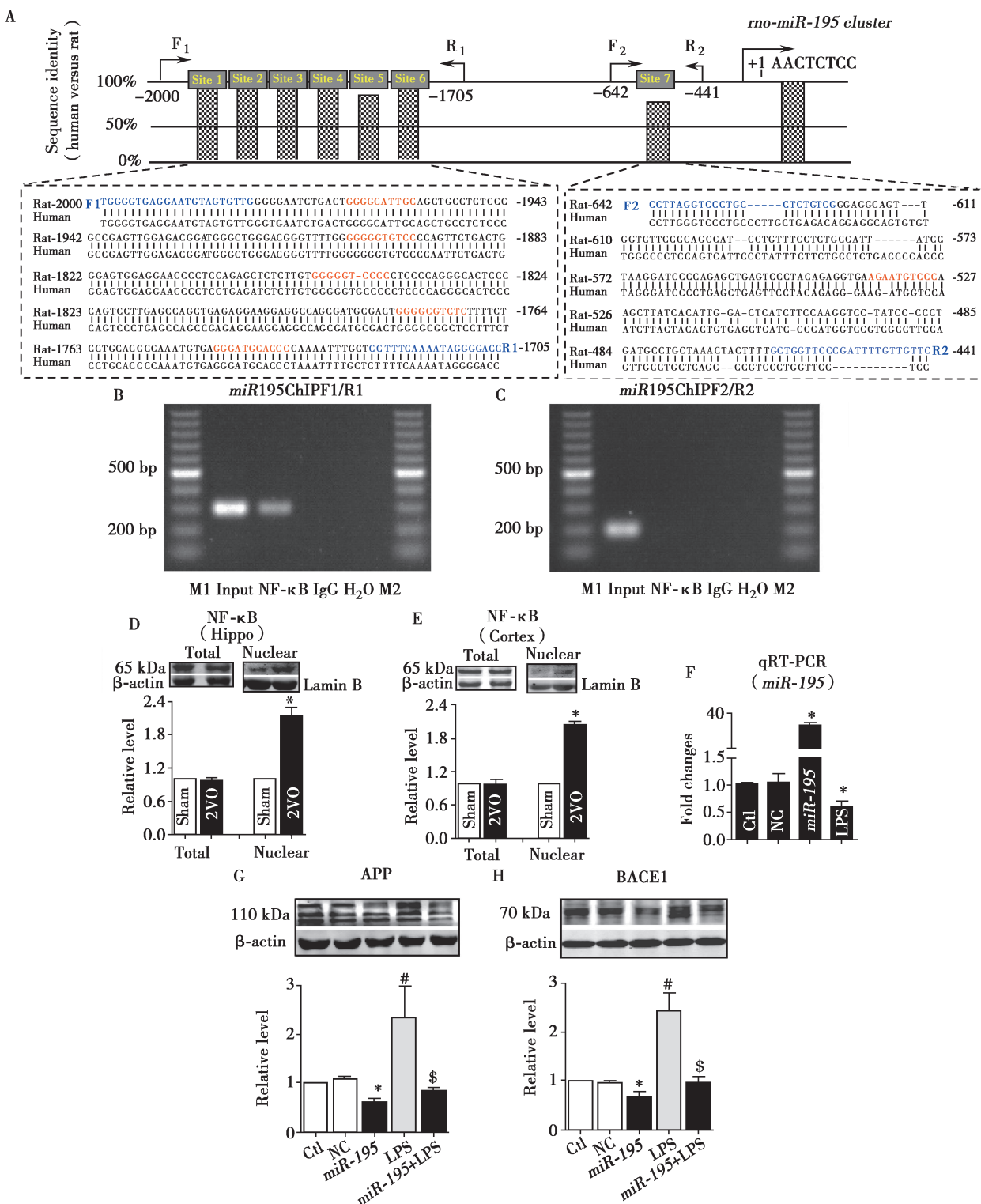


Fig. 6 NF-κB regulates *miR-195* cluster transcription<sup>[12]</sup>

A: Schematic representation of the 7 upstream region of the rat *miR-195* cluster, sequences between -2000 and -441 bp of the rat *miR-195* cluster are aligned with the corresponding sequences of human *miR-195* cluster. The conservative NF-κB targeting sites were shown in red. The primers for ChIP assay were in blue. B: ChIP analysis of *in vivo* showing that NF-κB binding to the promoter of *miR-195* between -2000 and -1705 bp and activates *miR-195* promoter activity. C: ChIP analysis of *in vivo* NF-κB binding to the promoter of *miR-195* between -642 and 441 bp did not activate *miR-195* promoter activity. D, E: Total and nuclear NF-κB protein expressions in hippocampus D and cortex E tissues of 2VO rats. F: LPS inhibited the expression of *miR-195* determined with qRT-PCR after *miR-195* mimics transfection. G, H: Upregulation of APP G and BACE1 H protein expressions induced by LPS, which was reversed by *miR-195* mimics transfection. \*P<0.05 vs NC, #P<0.05 vs *miR-195*, \$P<0.05 vs LPS,  $\bar{x} \pm s$ .

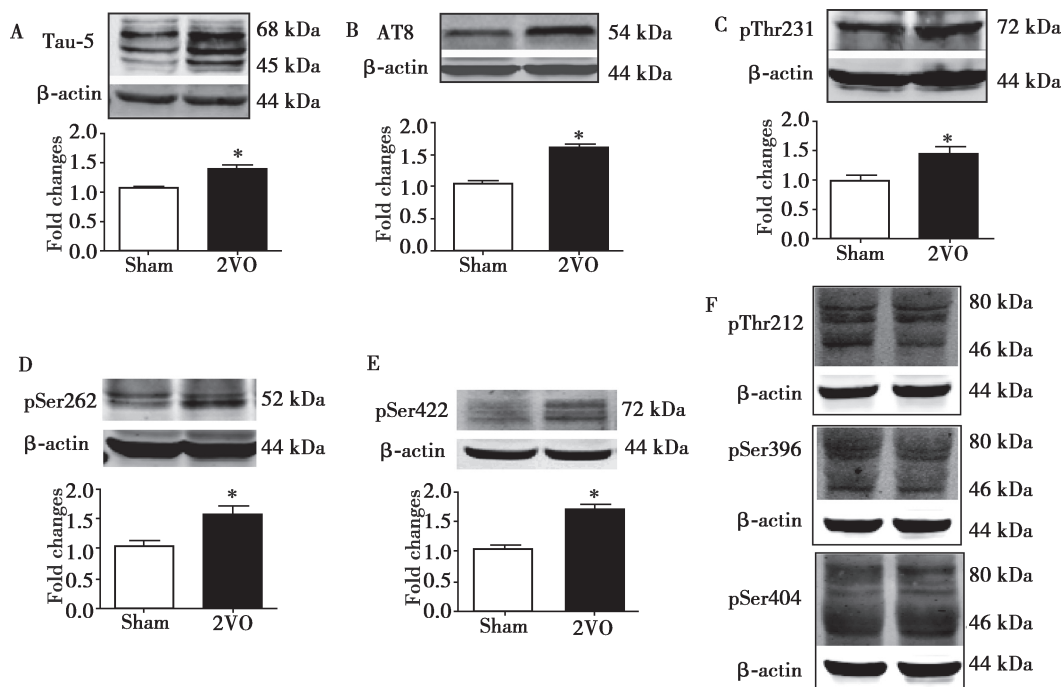


Fig. 7 Alterations in tau phosphorylation in the hippocampi of 2VO rats<sup>[15]</sup>

A: Increased expression of tau-5 in the hippocampi of 2VO rats compared to sham-operated rats. B~E: Elevated tau phosphorylation levels at sites of Ser202/Thr205 (AT8, B), Thr231 C, Ser262 D and Ser422 E. F: The level of tau phosphorylation was not changed at sites of Thr212, Ser396 and Ser404.  $\bar{x} \pm s$ , n = 6, \*P < 0.05 vs sham group.

calpain, 活化的 calpain 可以促进 CDK5/p35 (cyclin-dependent kinase 5) 转化成 CDK5/p25, 从而促进 tau 蛋白的磷酸化过程<sup>[14]</sup>。推测, miR-195 可能会通过促进 Aβ 的生成, 促进 CDK5/p35 向 CDK5/p25 的转化参

与 2VO 引起的 tau 蛋白过度磷酸化过程。课题组研究发现, 在 2VO 大鼠海马局部注射 lenti-pre-miR-195 可有效抑制 2VO 引起的 tau 蛋白 Ser202/Thr205 (AT8), Ser262 和 Thr231 位点的过度磷酸化 (Fig.8)。然而,

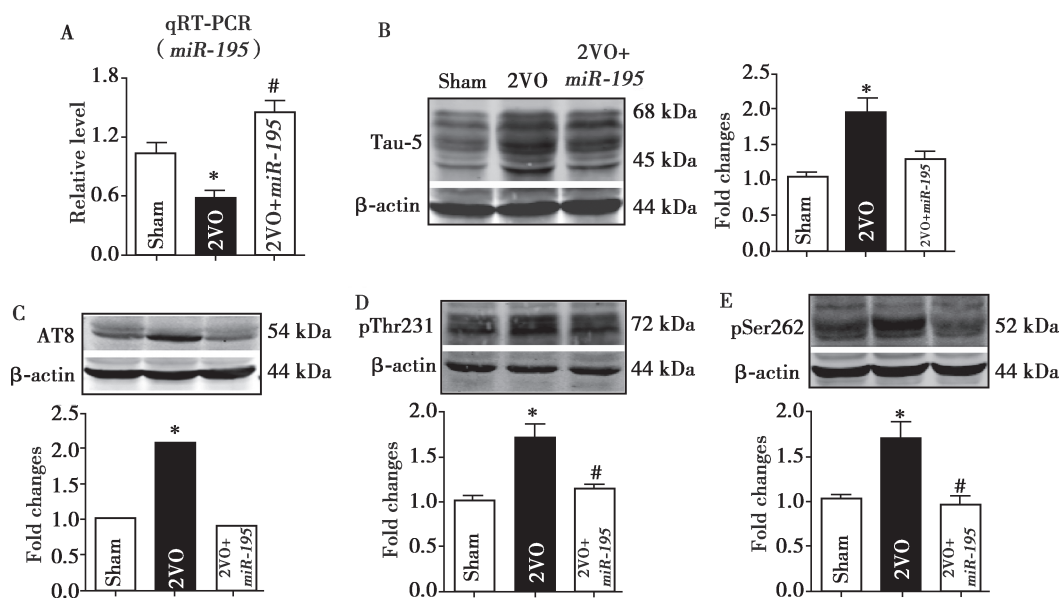


Fig. 8 miR-195 attenuates tau hyperphosphorylation in the hippocampi of 2VO rats<sup>[15]</sup>

A: Quantification of miR-195 in the hippocampi of 2VO rats with or without lenti-pre-miR-195 treatment as determined using qRT-PCR. B: Lenti-pre-miR-195 prevents the increase in tau-5 expression in the hippocampi of 2VO rats. C-E: miR-195 reverses the hyperphosphorylated tau in the hippocampi of 2VO rats at Ser202/Thr205 (AT8, C), Ser231 D and Thr262 E.  $\bar{x} \pm s$ , n = 6, \*P < 0.05 vs sham, #P < 0.05 vs 2VO.

与推测不同的是,虽然lenti-pre-*miR-195*干预促进了p25的表达,p35的水平并没有因为p25的升高而下降(Fig.9 A~C)。通过使用*miR-195*和AMO-195干预在体(Fig.9 D~F)和原代培养的神经元实验(Fig.9 G~I),课题组发现*miR-195*可以显著抑制p35的表达,这一作用可以被AMO-195所逆转,提示p35可能是*miR-195*的靶蛋白。随后,这一推论通过萤光素酶双报告基因技术得到证实(Fig.10)<sup>[15]</sup>。

以往文献报道,除Aβ外,CDK5、蛋白磷酸酶2A(protein phosphatase-2A, PP2A)和糖原合成激酶3β

(glycogen synthesis kinase 3β, GSK3β)也可以调节tau蛋白的磷酸化过程<sup>[16~17]</sup>。为此提出问题:PP2A和GSK3β是否参与了2VO引起的tau蛋白的磷酸化过程,如果参与其中,其与*miR-195*又有何关系?因此,本课题组进行了下列的研究。

众所周知,PP2A的活性主要依赖于PP2A翻译后修饰。PP2A催化亚基PP2A<sub>C</sub>在酪氨酸磷酸化位点p-Tyr307磷酸化水平和甲基化位点Leu309甲基化水平均可调节PP2A的活性(Fig.11A)<sup>[18]</sup>。p-Tyr307磷酸化水平增加和Leu309甲基化水平下降均预示着PP2A

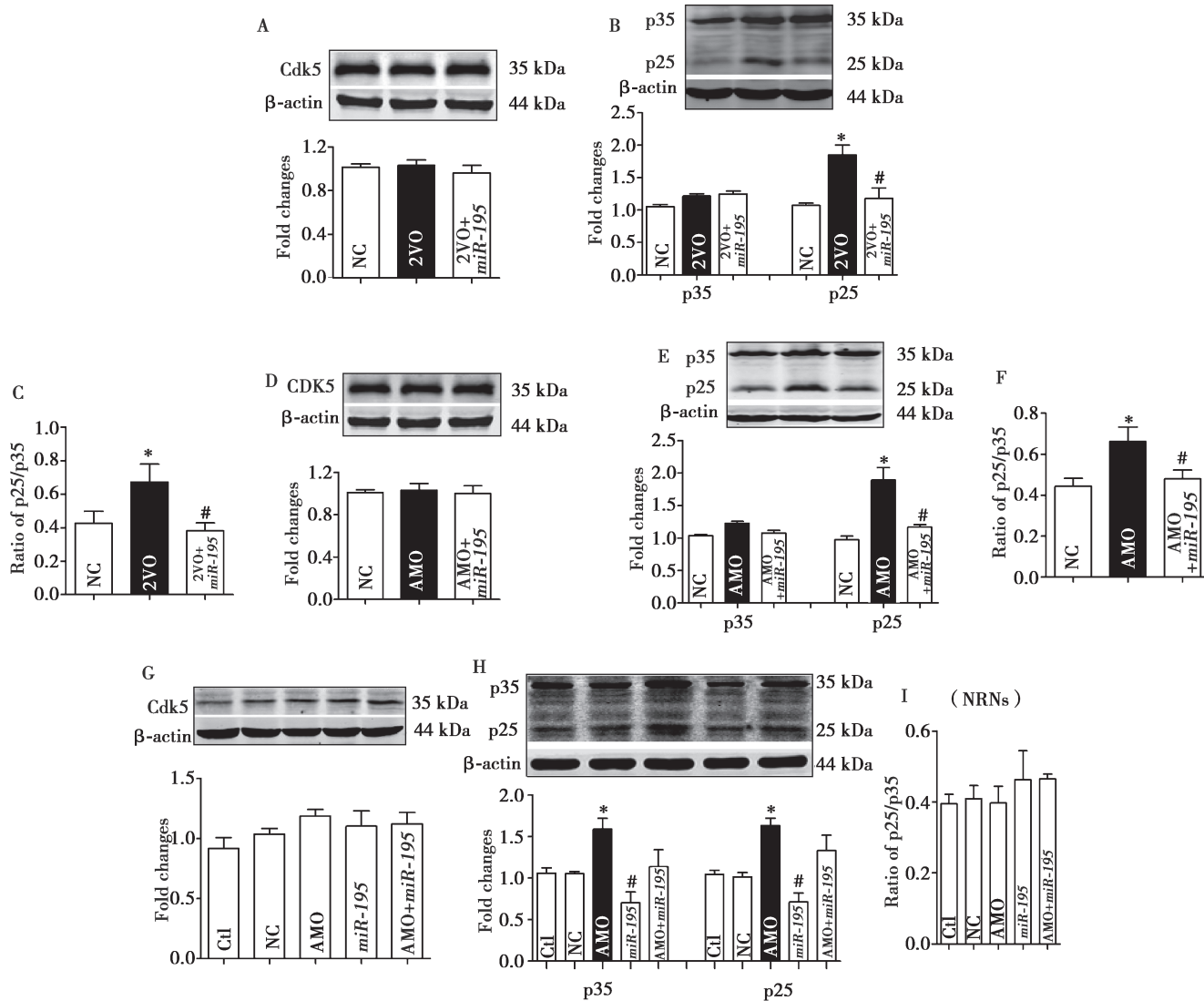


Fig. 9 Knockdown of *miR-195* induces the conversion of p35 to p25 and the generation of p35 in vivo and in vitro<sup>[15]</sup>

A: Lenti-pre-*miR-195* does not affect the expression of Cdk5 in the hippocampi of 2VO rats. B, C: Lenti-pre-*miR-195* prevents p25 accumulation B and the p25/p35 ratio increase C in the hippocampi of 2VO rats. D: Lenti-pre-*miR-195* does not affect the Cdk5 expression in the hippocampi of rats co-injected with lenti-pre-AMO-*miR-195*. E, F: Lenti-pre-*miR-195* prevents p25 accumulation E and the p25/p35 ratio increase F in the hippocampi of rats co-injected with lenti-pre-AMO-*miR-195*.  $\bar{x} \pm s$ ,  $n = 6$ , \* $P < 0.05$  vs NC, # $P < 0.05$  vs lenti-pre-*miR-195*. G: *miR-195* does not affect the expression of Cdk5 in primary cultured NRNs.  $\bar{x} \pm s$ ,  $n = 6$ . H: Effects of *miR-195* on the expression of p35 and p25 in primary cultured NRNs.  $\bar{x} \pm s$ , from 3 batches of cells for each group, \* $P < 0.05$  vs NC, # $P < 0.05$  vs AMO-195. I: *miR-195* does not affect the p25/p35 ratio in primary cultured NRNs.  $\bar{x} \pm s$ ,  $n = 6$ .

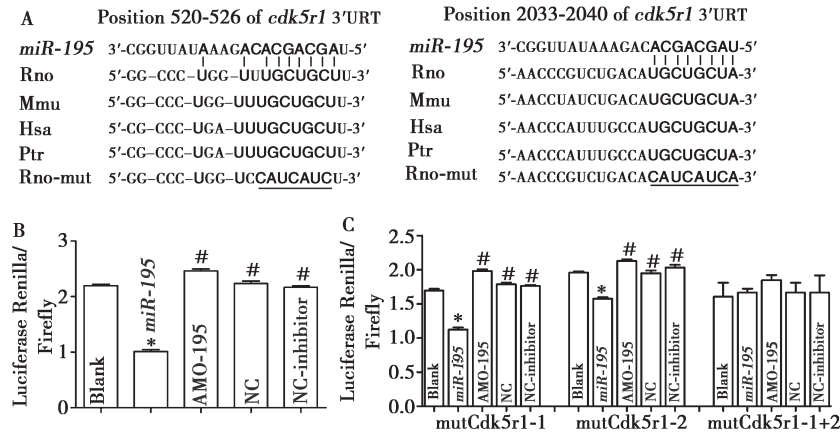


Fig. 10 *Cdk5r1* is a potential target of *miR-195* [15]

A: Complementarity between the *miR-195* seed sequence (5' end, 7-8 nucleotides) and the 3'UTR of the rat p35 predicted using a computational and bioinformatics-based approach using the Targetscan algorithm. Watson-Crick complementarity is indicated by “|” connections. The mutations made to the genes are underlined. B, C: Luciferase reporter gene assay for interactions between *miR-195* and its binding sites B or mutation of binding sites C in the 3'UTR of the *Cdk5r1* gene in HEK293T cells.  $\bar{x} \pm s$ , from 3 batches of cells for each group, \* $P < 0.05$  vs blank, # $P < 0.05$  vs *miR-195*.

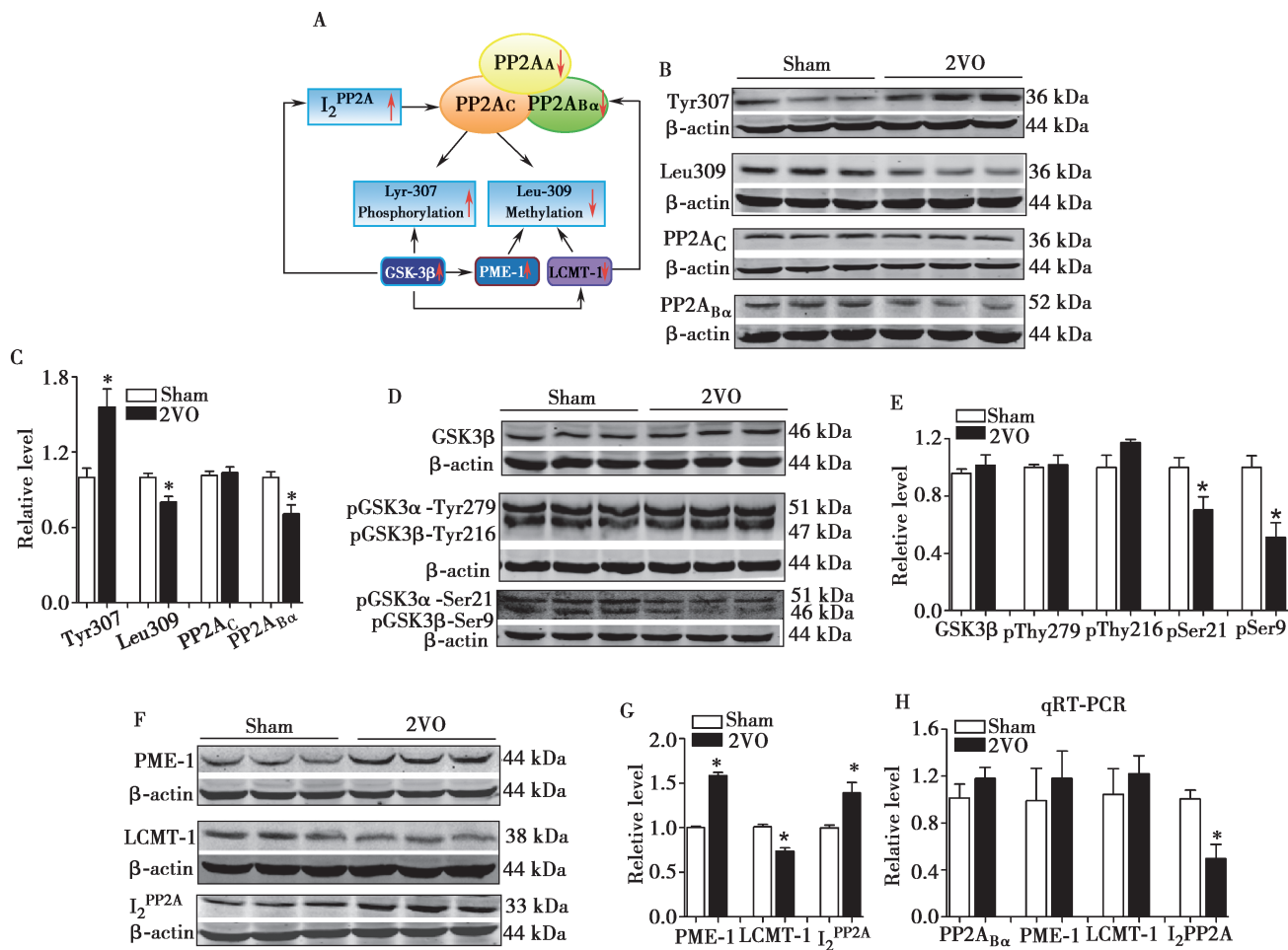


Fig. 11 Reduction of PP2A activities in the hippocampi of 2VO rats [23]

A: Schematic diagram of the regulation of PP2A activity. B: Changes in the levels of PP2A activity associated proteins in the hippocampi of 2VO rats including Tyr307, Leu309, PP2A<sub>C</sub>, and PP2A<sub>B $\alpha$</sub> . C: Statistical analysis of Tyr307, Leu309, PP2A<sub>C</sub>, and PP2A<sub>B $\alpha$</sub>  expression. D, E: GSK3 $\beta$  and its activity in the hippocampi of 2VO rats compared to sham-operated rats.  $\bar{x} \pm s$ ,  $n = 6$ , \* $P < 0.05$  vs sham group. F~H: Alteration in PME-1, LCMT-1 and  $I_2^{PP2A}$  expression in the hippocampi of 2VO rats. PP2A<sub>B $\alpha$</sub> , PME-1, LCMT-1 and  $I_2^{PP2A}$  mRNA levels in the hippocampi of 2VO rats determined using qRT-PCR.

活性的下降<sup>[19-20]</sup>。研究发现,2VO大鼠海马 p-Tyr307 磷酸化水平明显增加,而 Leu309 甲基化水平明显下降,提示 2VO 大鼠海马组织 PP2A 活性下降(Fig.11B,C)。有文献报道,GSK3β 激酶的激活参与 p-Tyr307 磷酸化水平增加过程和 Leu309 甲基化水平下降过程,对 PP2A 活性调节具有一定作用(Fig.11A)<sup>[21]</sup>。本课题组的研究结果显示,与假手术组相比,2VO 大鼠海马 GSK3β 总蛋白、pGSK3α-Tyr297 和 pGSK3β-Tyr216 磷酸化水平无明显变化,但是 pGSK3α-Ser21 和 pGSK3β-Ser9 磷酸化水平明显下降(Fig.11D,E),结果说明,在 2VO 模型中,激活的 GSK3β 激酶参与 CBH 情况下 PP2A 的失活。

那么,2VO 又是如何调节 PP2A 的活性?已知,PP2A 甲基酯酶 1(methylesterase 1, PME-1)上调、PP2A 甲基转移酶 1(leucine carboxyl methyltransferase-1, LCMT-1)下调和 PP2A 内源性抑制剂 2(endogenous nuclear inhibitor 2, I<sub>2</sub><sup>PP2A</sup>)的上调均会使 Leu309 甲基化水平下降(Fig.11A)<sup>[19,20,22]</sup>。进一步的研究显示,2VO 模型组 PME-1 蛋白表达量显著增加,LCMT-1 蛋白表达量有所下降,PP2A 内源性抑制剂 I<sub>2</sub><sup>PP2A</sup> 蛋白表达量也显著增加(Fig.11F,G)。qRT-PCR 分析显示,2VO 模

型组 PP2A<sub>B<sub>α</sub></sub>,PME-1 和 LCMT-1 蛋白 mRNA 水平与假手术组相比无明显变化,而 I<sub>2</sub><sup>PP2A</sup> 蛋白 mRNA 则显著下降(Fig.11H),提示 PME-1 和 LCMT-1 存在转录后调节的机制。那么,这种转录后调节的过程与 miR-195 有何关系?本课题组采用与前期相同的研究策略,发现向 2VO 大鼠海马局部注射 lenti-pre-miR-195 可以有效逆转 2VO 引起的 PME-1 升高和 LCMT-1 的下降,但是不影响 I<sub>2</sub><sup>PP2A</sup> 蛋白的水平(Fig.12 A-C)。有趣的是,发现 2VO 引起的 LCMT-1 的变化与 miR-195 下调引起的 A<sub>β</sub> 沉积有关,但是屏蔽 miR-195 与 APP 和 BACE1 基因的结合位点并不影响 PME-1 的变化(Fig.12 D-F)。随后研究发现,编码 PME-1 的基因 Ppme1 是 miR-195 的靶基因(Fig.13 A-F)。

综合以上研究结果,发现 CBH 可以通过激活 CDK5 和 GSK3β,抑制 PP2A 活性促进大鼠海马区 tau 蛋白过度磷酸化。2VO 引起的 miR-195 下调通过转录后调节机制上调 APP 和 BACE1 的表达生成 A<sub>β</sub>,促进 CDK5/p35 向 CDK25/p25 的转化和 LCMT-1 的表达而增加 tau 蛋白的磷酸化,同时又直接调节其靶蛋白 CDK5/p35 和 PME-1 表达,提供增加 tau 蛋白磷酸化的底物蛋白<sup>[23]</sup>。

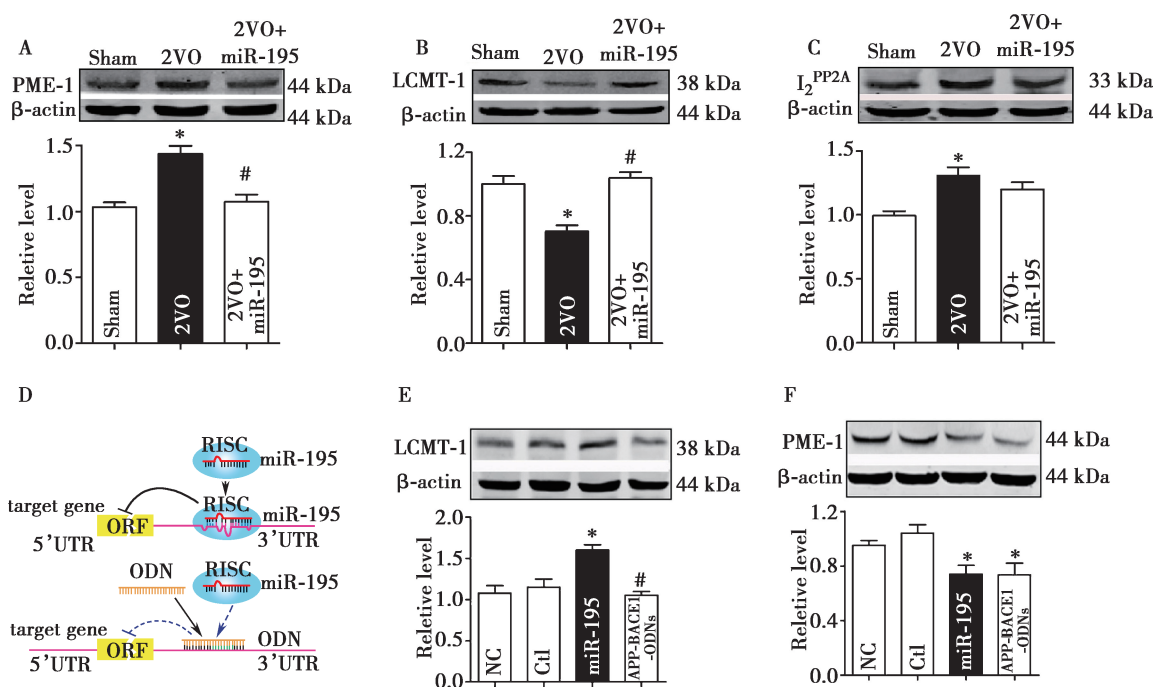
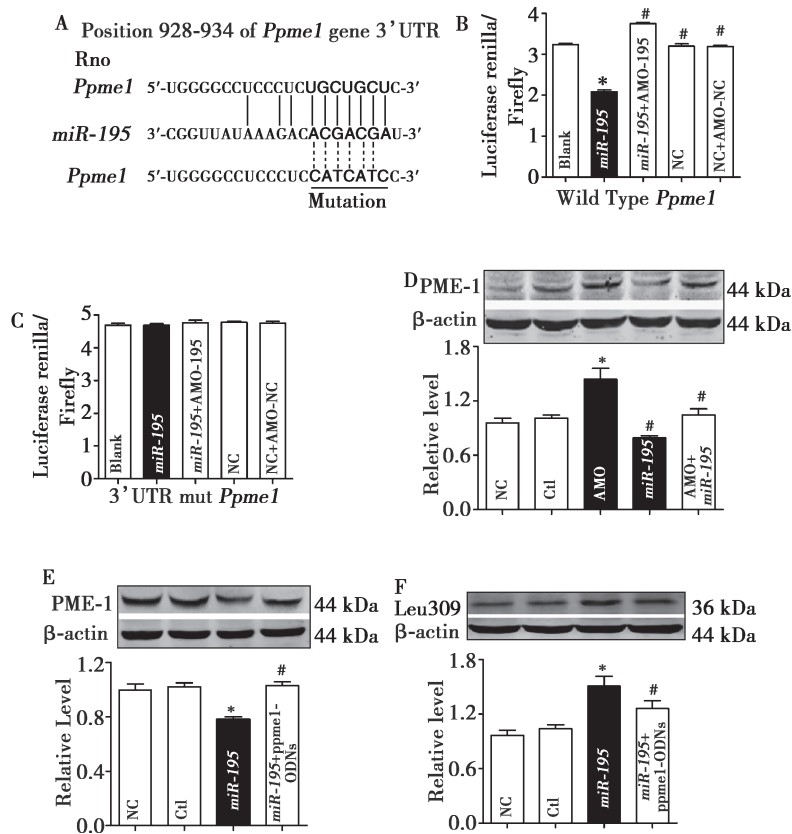


Fig. 12 Effects of miR-195 on the regulators of PP2A activity in vivo<sup>[23]</sup>

A-C: Lenti-pre-miR-195 injection prevents the PME-1 increase A and LCMT-1 reduction B without affecting the increased in the I<sub>2</sub><sup>PP2A</sup> level C in the hippocampi of 2VO rats. D:Schematic of miR-195 silencing using ODNs. Gene-specific ODNs, designed as 22 oligonucleotides fully complementary to the complete sequence of miR-195 target sites in the 3'UTRs of APP or BACE1, has high binding affinity and completely masks the target sites of miR-195 in the 3'UTRs of APP or BACE1. ORF, open reading frame. E: APP-ODN and BACE1-ODNs attenuate the facilitative effects of miR-195 on LCMT-1 expression.F APP-ODN and BACE1-ODNs does not change PME-1 decrease induced by miR-195 in NRNs.  $\bar{x} \pm s$ , from 3 batches of cells for each group, \*P < 0.05 vs NC, #P < 0.05 vs miR-195.



**Fig. 13 The *Ppme1* gene is a potential target of miR-195<sup>[23]</sup>**

A: Complementarity between the miR-195 seed sequence (5' end, 7-8 nucleotides) and the 3'UTR of rat *Ppme1* predicted using the Targetscan algorithm. Watson-Crick complementarity is indicated by “|” connections. The mutations introduced into the genes are underlined. B, C: Luciferase reporter gene assay to detect interactions between miR-195 and its binding sites B or mutation of binding sites C in the 3'UTR of the *Ppme1* gene in HEK293T cells.  $\bar{x} \pm s$ , from 3 batches of cells per group, \* $P < 0.05$  vs blank, # $P < 0.05$  vs miR-195. D: miR-195 inhibits the increase in PME-1 expression in NRNs after AMO-195 transfection. E, F: the *Ppme1*-ODN diminished the inhibitory effect of miR-195 on PME-1 protein expression E and the facilitative action of miR-195 on Leu309 methylation F.  $\bar{x} \pm s$ , from 5 batches of cells per group, \* $P < 0.05$  vs NC, # $P < 0.05$  vs miR-195.

### 3 miR-195 参与 CBH 引起的神经元树突退化和神经元的死亡

除 A $\beta$  沉积和 tau 蛋白过度磷酸化以外, 神经元丢失引起的脑萎缩和神经元突触退化是痴呆患者尸检发现的另一重要病理特征<sup>[24]</sup>。A $\beta$  沉积和 tau 蛋白过度磷酸化均可以引起神经元死亡<sup>[25]</sup>。那么, CBH 是否会引起大鼠海马和皮层神经元退变及神经元丢失, miR-195 是否参与其中并不清楚。为了探讨这个问题, 采用 2VO 动物模型, 运用经典的高尔基染色观察树突的变化, Nissl 和 TUNEL 染色观察神经元的死亡和凋亡。研究结果表明: 与假手术组相比, 2VO 组大鼠海马和皮层区锥体及颗粒神经元的树突总长度、总数量、sholl 分析交叉点数均显著降低 (Fig.14 A~P), 并且神经元死亡显著增加 (Fig.14 Q, R)。Nikolaev 等研究发现, 在神经营养因子剥夺的神经元中, 作为 A $\beta$  生成的代谢产物, 氨

基端淀粉样前体蛋白 (N-terminal  $\beta$ -amyloid precursor protein, N-APP) 能够和死亡受体 6 (death receptor-6, DR6) 结合, 触发神经元轴突的退化和胞体的凋亡, 且这一过程分别需要凋亡蛋白 caspase 6 和 caspase 3 的参与<sup>[26]</sup>。利用免疫荧光染色技术研究发现, 与假手术组相比, 2VO 组大鼠海马和皮层区中裂解的 caspase 6 和 caspase 3 的染色均显著增强 (Fig.15 A, B), 说明 2VO 组大鼠海马和皮层区的 caspase 6 和 caspase 3 被明显激活。有趣的是, Western blot 检测表明 2VO 组大鼠海马和皮层区不仅表现为 N-APP 的升高 (Fig.15C), DR6 蛋白表达也明显升高 (Fig.15D)。进一步研究发现, DR6 是 miR-195 的靶蛋白, miR-195 可以转录后调节 DR6 表达 (Fig.16 A~F)。同样, 向 2VO 大鼠海马局部注射 lentiviral-pre-miR-195 显著缓解 2VO 引起的 N-APP 和 DR6 蛋白表达的变化 (Fig.17A~C) 以及神经元树突退化和神经

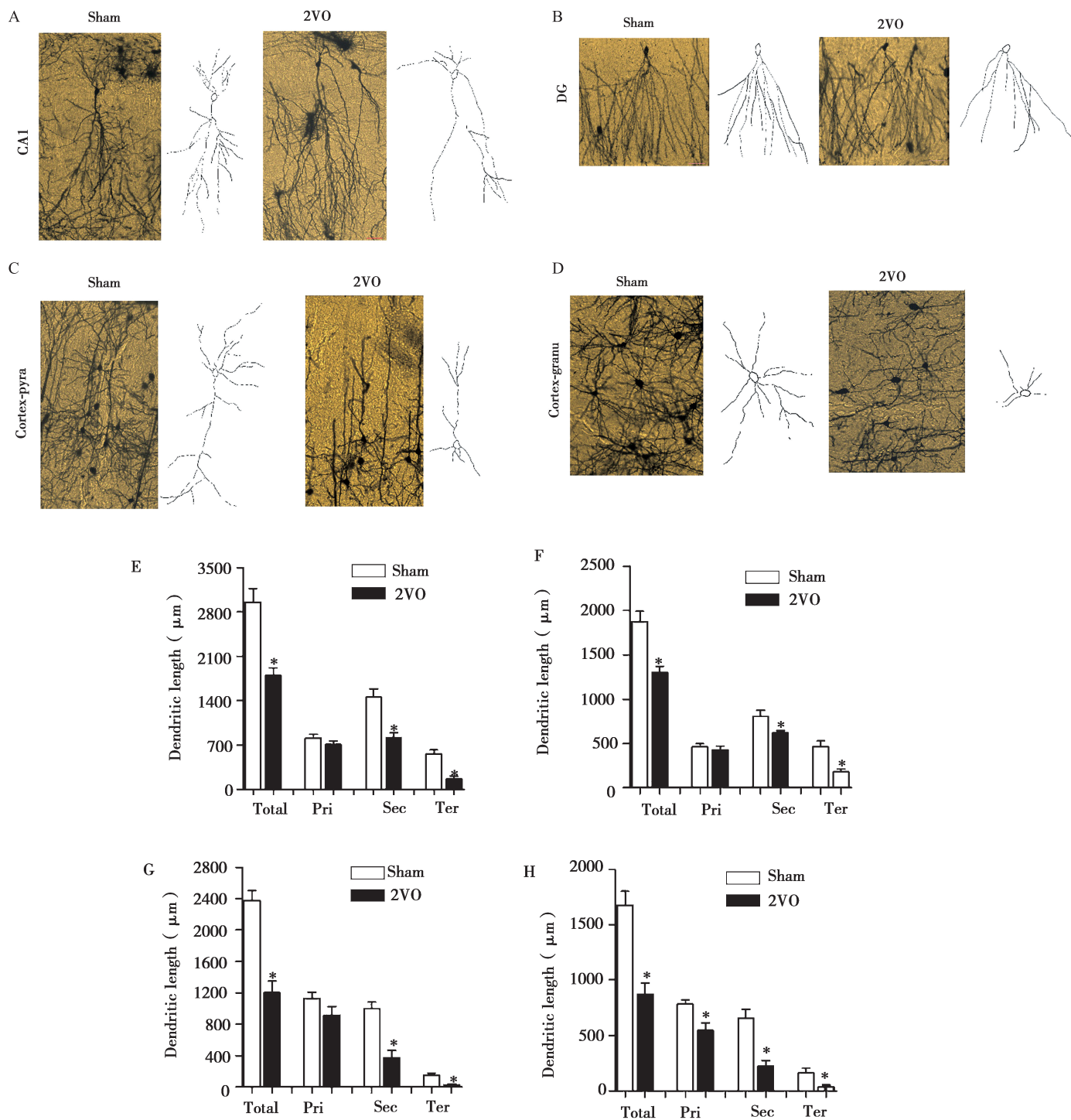


**Fig. 14 Dendritic complexity deficits and neuron loss in hippocampi and cortices of 2VO rats<sup>[27]</sup>**

A~D: Representative photomicrographs (left) and tracing images (right) of dendritic arborization in hippocampal CA1 pyramidal neurons A, DG granular neurons B, cortical pyramidal neurons C, and cortical granular neurons D from sham and 2VO rats. E~H: Quantification of the length of dendrites in hippocampal CA1 pyramidal neurons E, DG granular neurons F, cortical pyramidal neurons G, and cortical granular neurons H.

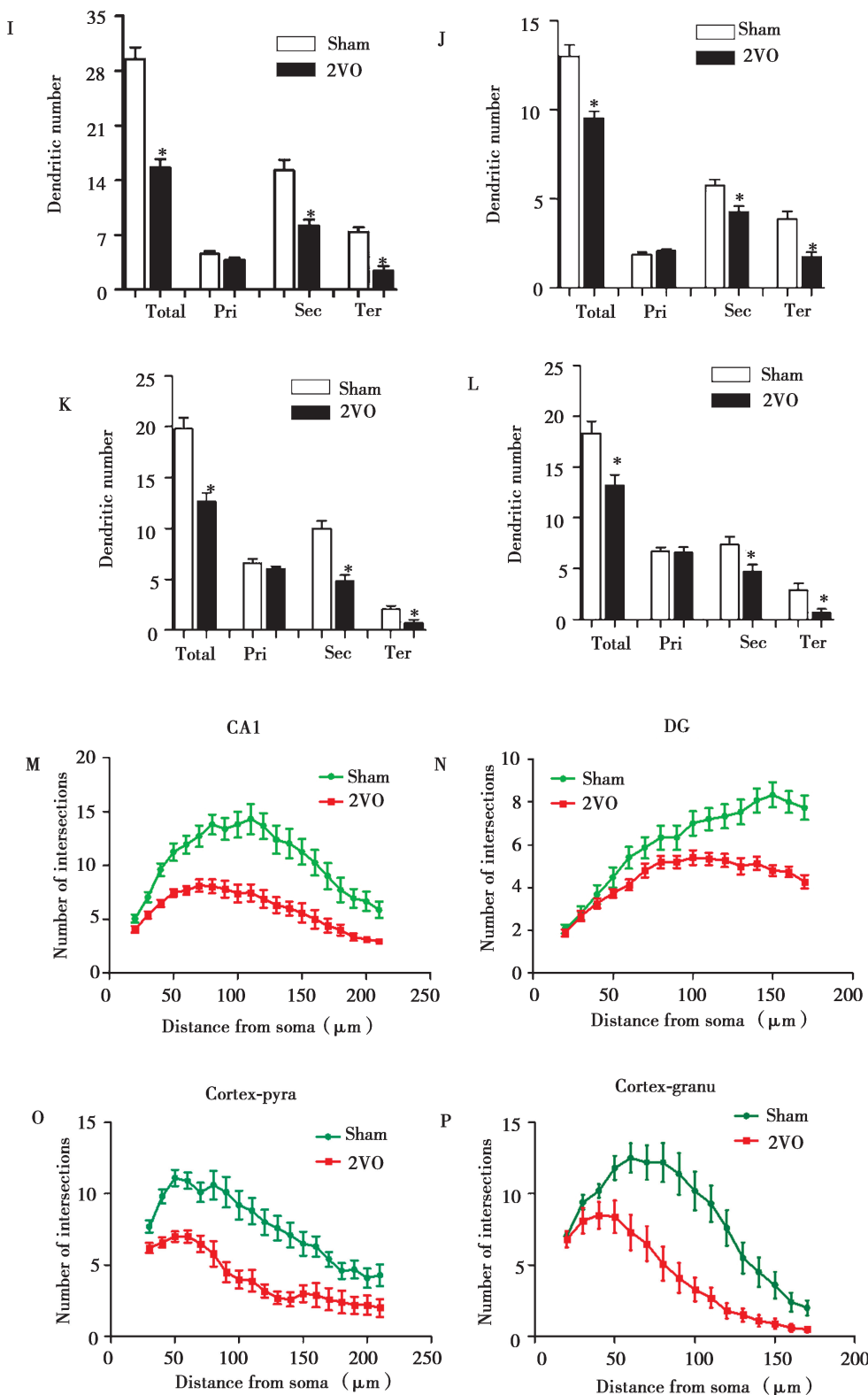


Fig. 14 (continued)

I~L: Quantification of the number of dendrites in hippocampal CA1 pyramidal neurons I, DG granular neurons J, cortical pyramidal neurons K, and cortical granular neurons L. M~P: Sholl analysis of the number of intersections of dendrites in hippocampal CA1 pyramidal neurons M, DG granular neurons N, cortical pyramidal neurons O, and cortical granular neurons P. (Data are reported as the  $\bar{x} \pm s$ ,  $n = 15$ . \* $P < 0.05$  vs sham. Abbreviations: Total, total dendrite; Pri, primary dendrite; Sec, secondary dendrite; Ter, tertiary dendrite).

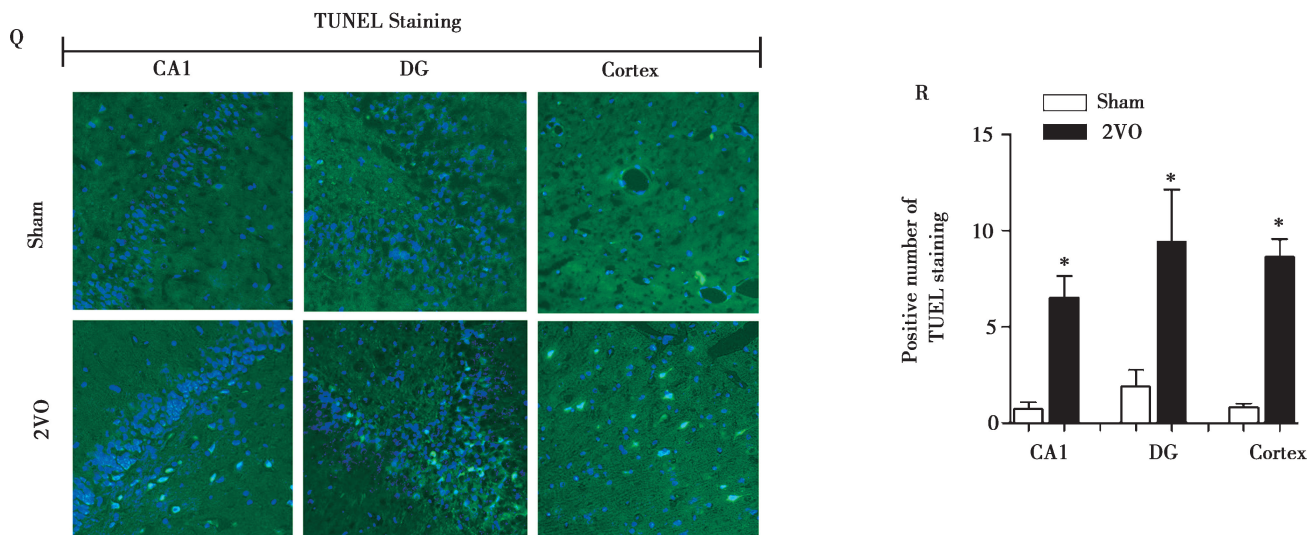


Fig. 14 (continued)

Q: Representative TUNEL photomicrographs in hippocampal CA1 and DG and cortex of sham and 2VO rats at 20 $\times$  magnification. R: Statistical analysis of TUNEL-positive cells in hippocampal CA1 and DG and cortex of sham and 2VO rats.  $\bar{x} \pm s$ , n = 5, \*P < 0.05 vs sham.

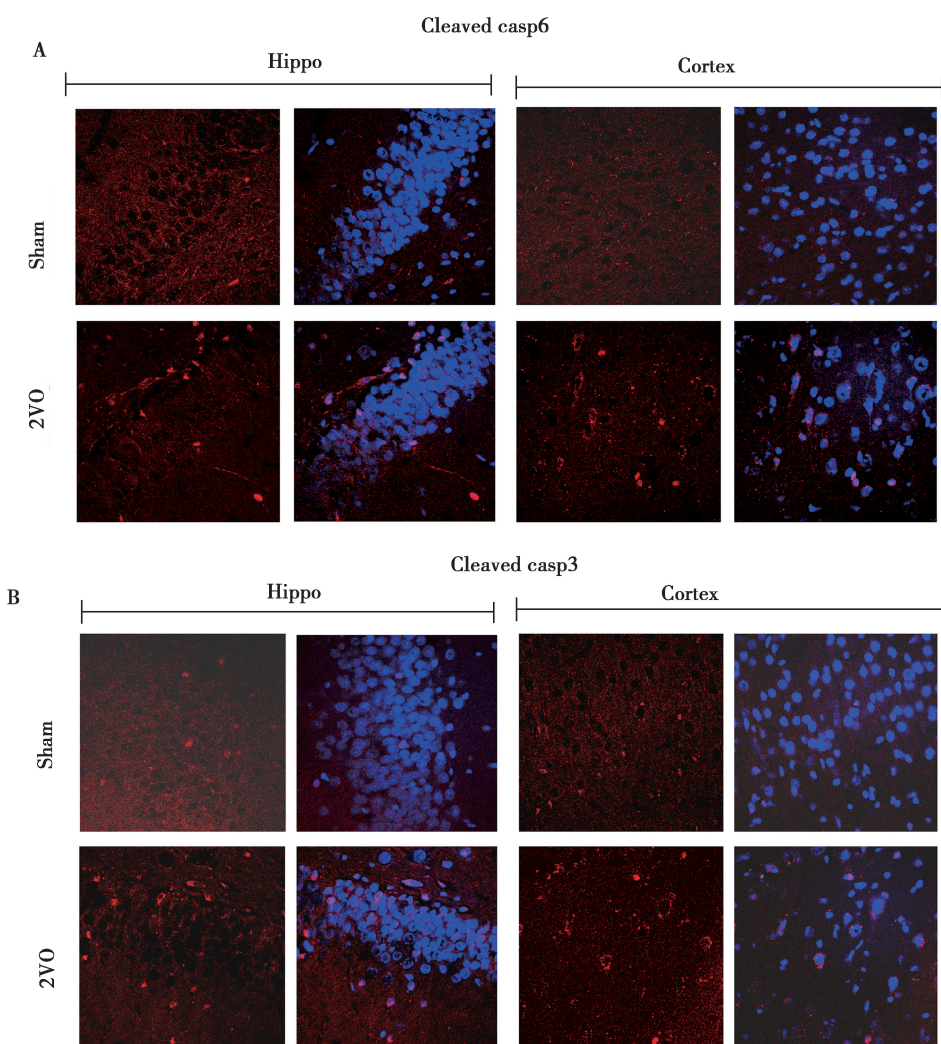


Fig. 15 2VO activates the N-APP/DR6/caspase pathways in rats<sup>[27]</sup>

A, B: Activated caspase-6 (A, red) and caspase-3 (B, red) in the hippocampi and cortices of 2VO rats shown by immunofluorescence staining. (nuclei are labeled with blue DAPI, and the magnification is 20 $\times$ ).

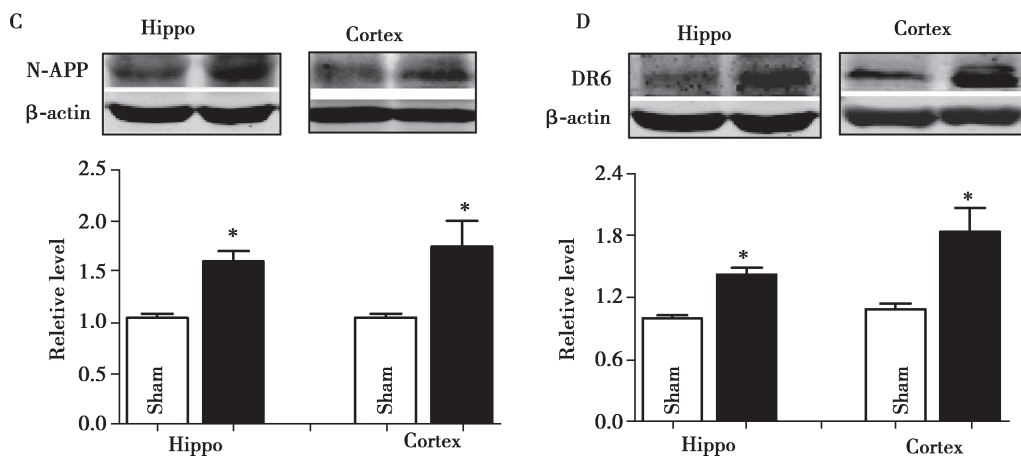


Fig. 15 (continued)

C~D: CBH upregulated N-APP and DR6 expression in rat hippocampi and cortices.  $\bar{x} \pm s$ ,  $n = 6$ , \* $P < 0.05$  vs sham.

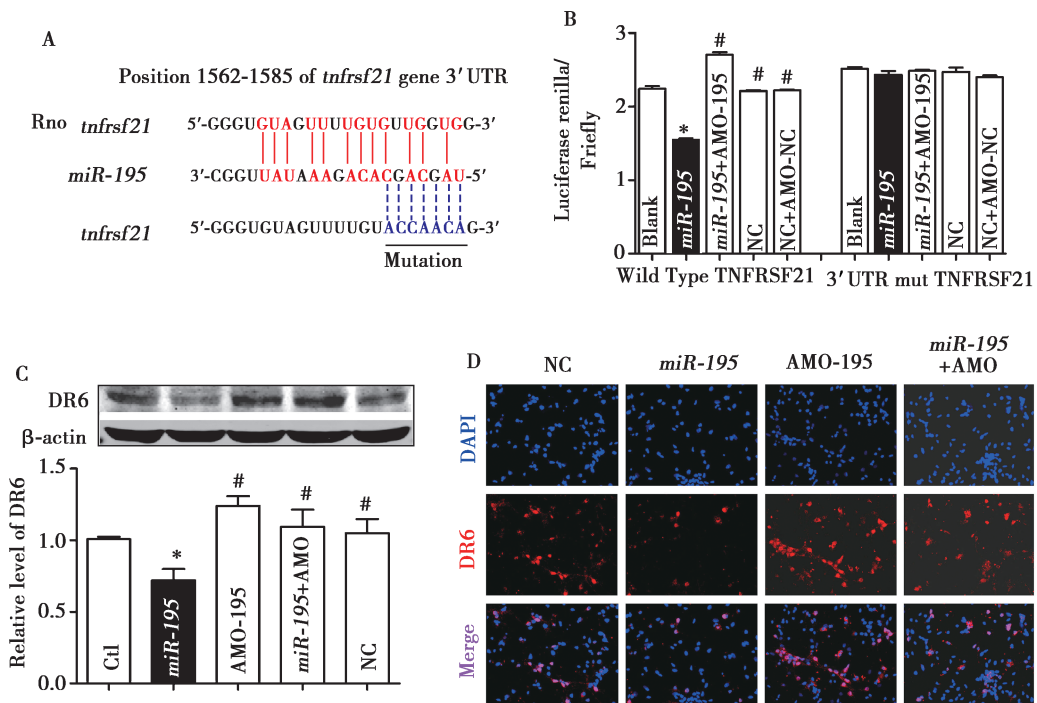


Fig. 16 DR6 is a direct target of *miR-195* [27]

A: Schematic of the predicted *miR-195* binding site in the DR6 3'UTR in rats. Nucleotides with Watson-Crick complementarity are connected by “|”. The mutations made to the genes are underlined. B: A luciferase reporter gene assay detected the direct interaction between *miR-195* and its binding sites in the 3'UTR of the DR6 mRNA in HEK293T cells. \* $P < 0.05$  vs blank, # $P < 0.05$  vs *miR-195*. C, D: The effects of *miR-195* on endogenous DR6 expression in NRNs by Western blotting and immunofluorescence staining after the neurons were transfected with *miR-195*, *AMO-195*, *miR-195 + AMO-195*, or *NC*.

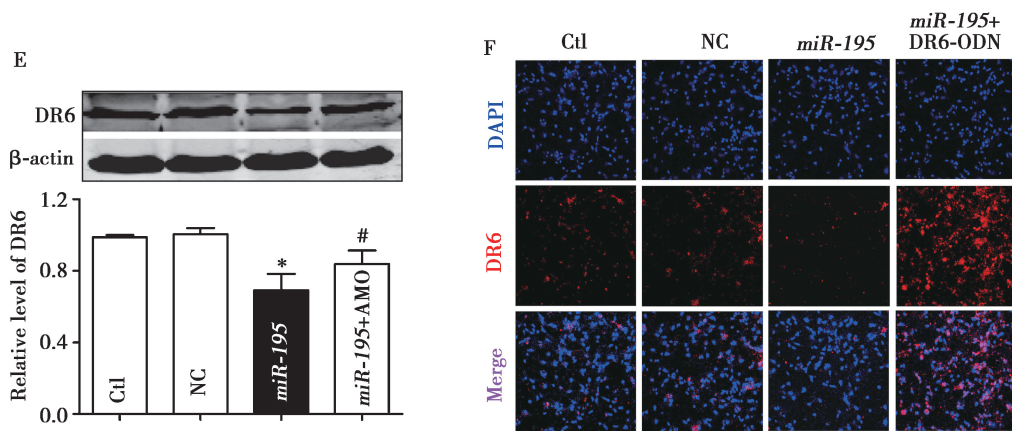


Fig. 16 (continued)

E, F: Depression of DR6 by DR6-ODN in NRNs, determined by Western blotting and immunofluorescence staining.  $n = 6$ , \* $P < 0.05$  vs control, # $P < 0.05$  vs miR-195. Representative photomicrographs are at a magnification of  $20 \times$ .

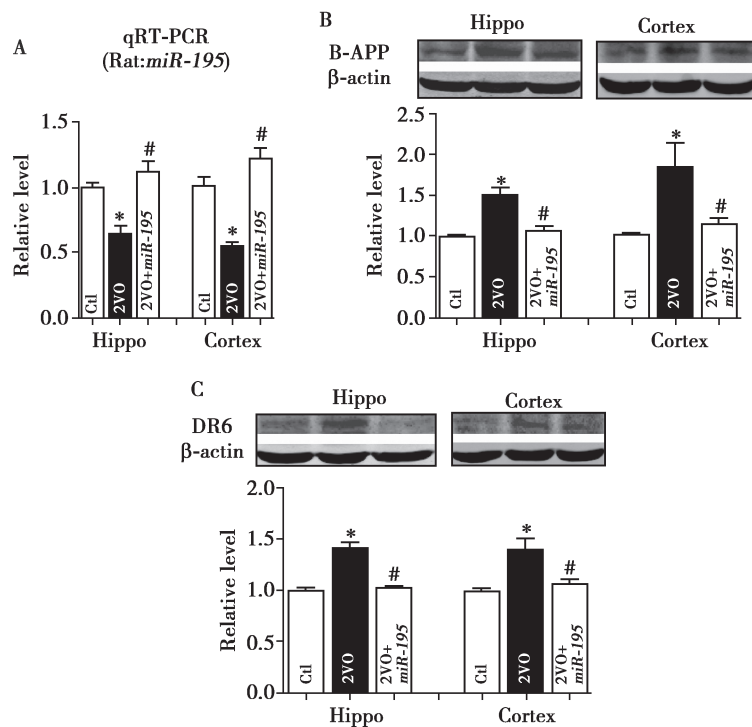


Fig. 17 Overexpression of miR-195 prevents 2VO-induced activation of the N-APP/DR6/caspase pathway<sup>[27]</sup>

A: miR-195 levels in the hippocampi and cortices of 2VO rats with or without lenti-pre-miR-195 treatment. B, C: Lenti-pre-miR-195 prevented the increase of N-APP and DR6 expression in the hippocampi and cortex of 2VO rats.  $\bar{x} \pm s$ ,  $n = 6$ , \* $P < 0.05$  vs sham, # $P < 0.05$  vs 2VO.

元的死亡(Fig.18A~J)。这些研究结果说明,在CBH状态下,下降的miR-195不仅通过促进A $\beta$ 及代谢产物N-APP的生成触发神经元树突退化和神经元死亡过程,而且同时上调DR6蛋白表达,为N-APP发挥作用提供充足的受体,为实现这一病理过程提供保障<sup>[27]</sup>。

#### 4 小结

A $\beta$ 沉积导致的老年斑,tau蛋白过度磷酸化引起的神经纤维缠结和神经元死亡引发的脑萎缩是老年痴呆患者3个标志性的病理改变,也被认为是导致患者发生学习记忆和认知功能下降的重要原因<sup>[28]</sup>。众多研究结果发现三者之间表现为错综复杂的互为因果关系,提示针对单一靶点的药物干预可能会是一个“一叶障目”的治疗策略。此外,值得关注的是,临床研究发现在患者被诊断为痴呆之前15~20年就已经观察到老年斑和脑萎缩,提示试图通过去改变一个陈旧性的病理变化来达到治疗目的似乎是一个“亡羊补牢”的方案。而不断失败的新药临床试验,也让全世界该领域的科学家意识到寻找针对多靶点早期干预措施可能是走出目前困境的有效途径<sup>[29]</sup>。本系列研究试图从CBH这一发生在AD和VD早期的病理生理过程结合

miRNAs的多靶点调控的特征去探讨是否有一个共调节因子通过调节3个病理生理过程参与VD学习记忆和认知功能下降的过程。本课题组发现,在CBH的条件下,miR-195并不是简单地参与了3个病理过程,而是表现为明显的规律性,也就是说2VO引起的miR-195下调不仅可以通过上调APP和BACE1的表达从源头启动A $\beta$ 级联反应过程,并且在这个级联反应过程的每一个关键节点处为维持反应过程提供底物(Fig.19)。这一研究结果说明尽管A $\beta$ 沉积、tau蛋白过度磷酸化和神经元死亡是老年痴呆尸检中发现的三个独立的病理特征,这三个病理特征其实存在内在统一的调节因子把三个病理特征连接到一个级联反应的过程,并使三个病理过程存在互为反馈的调节关系。同时,本课题组的研究也为目前用单一靶点进行干预进入临床试验的药物最终以失败告终的可能原因提供了基础证据。本系列研究也从另外一个角度证明miRNAs是可以在一个功能模块中以多靶点调控的方式参与到疾病的发生和发展过程中。然而,miR-195是否最终能够成为预测或者干预的靶点还有待于进一步的深入研究。miR-195是否还可以通过作用于其他的分子靶标参与学习和记忆的过程,我们拭目以待。

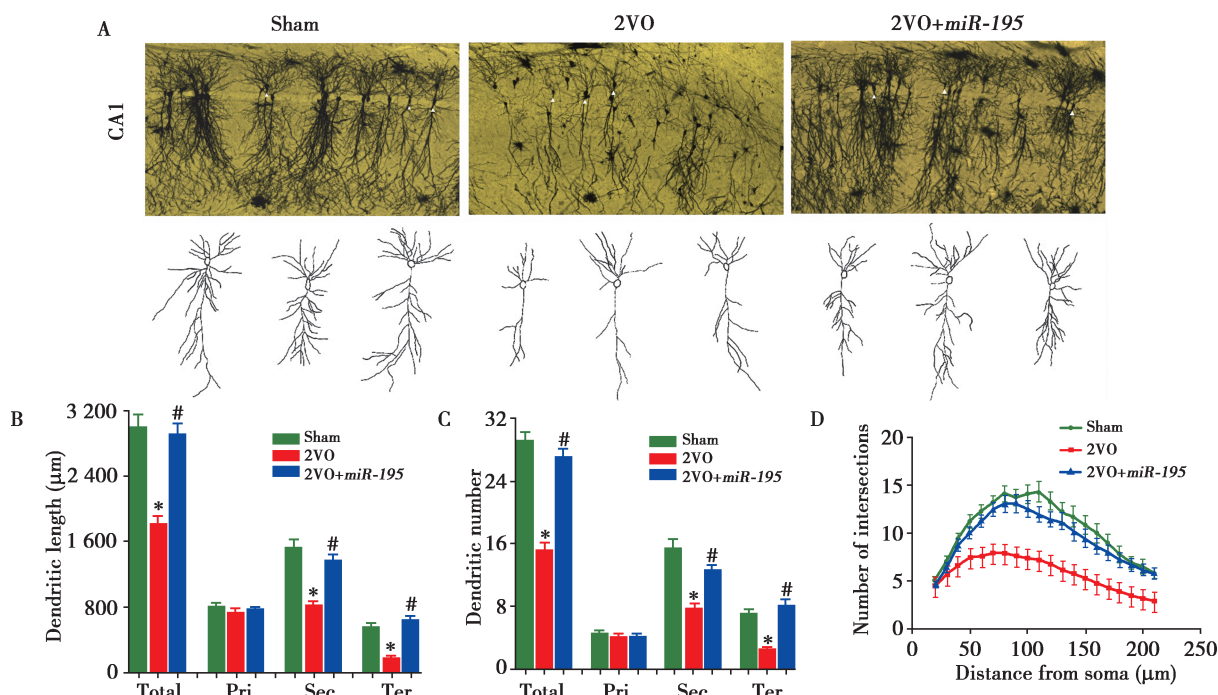


Fig. 18 miR-195 attenuates dendritic complexity deficits and neuron loss in 2VO rats<sup>[27]</sup>

A: Typical photomicrographs (top) and tracing images (bottom) of dendritic arborization in hippocampal CA1 pyramidal neurons of 2VO rats with or without lenti-pre-miR-195 treatment. B~D: Quantification of the length, the number and the intersection number of dendrites in hippocampal CA1 pyramidal neurons.

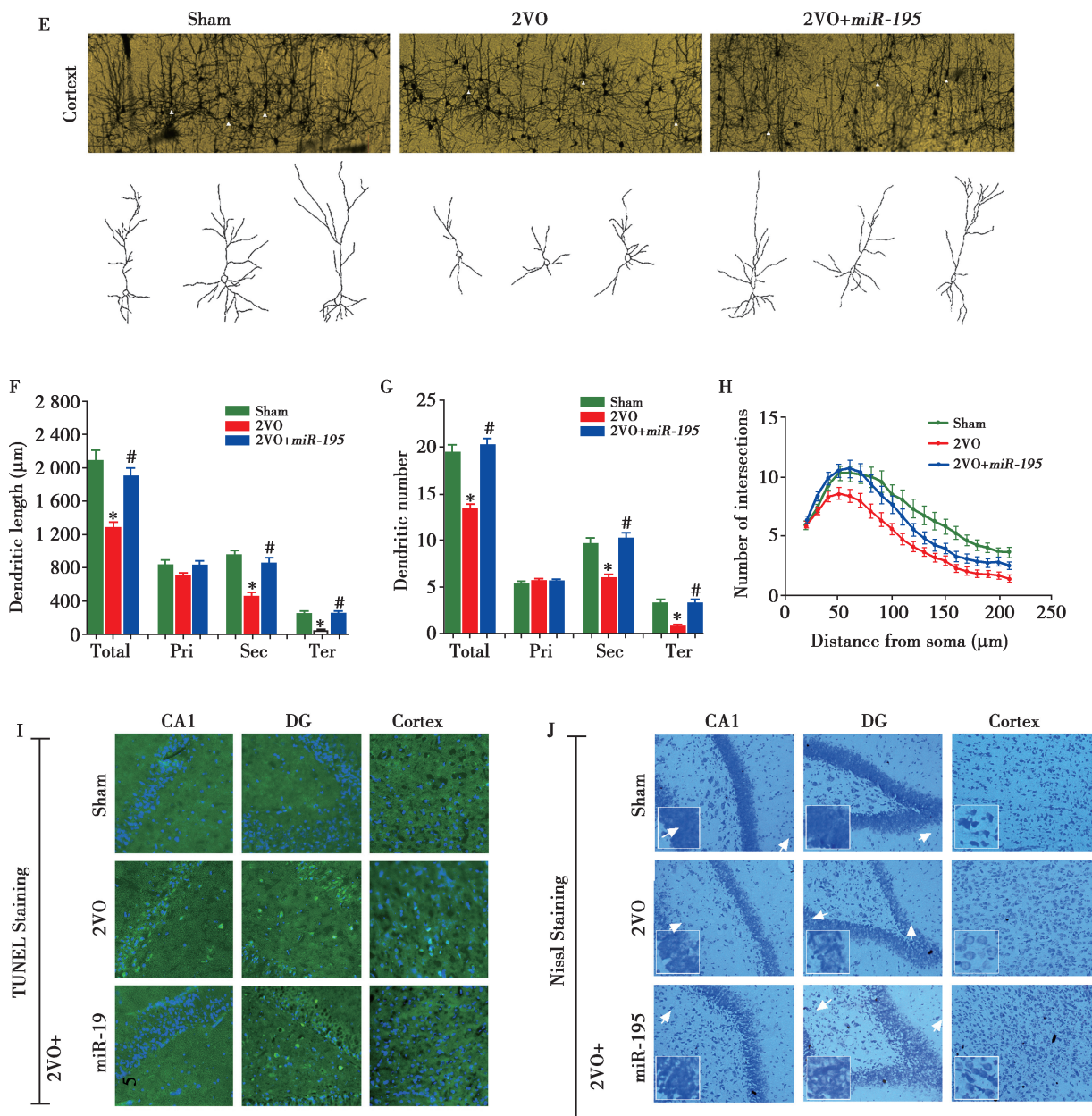
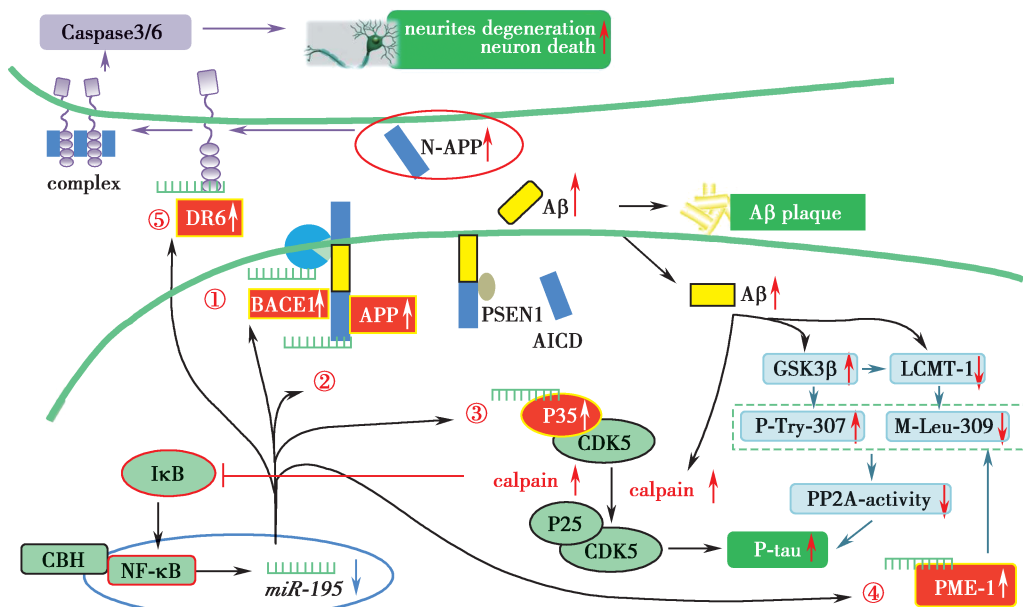


Fig. 18 (continued)

E: Typical photomicrographs (top) and tracing images (bottom) of dendritic arborization in cortical pyramidal neurons of 2VO rats with or without lenti-pre-*miR-195* treatment. F~H: Quantification of the length, the number and the intersection number of dendrites in cortical pyramidal neurons. ( $\bar{x} \pm s$ ,  $n = 20$  in hippocampi,  $n = 30$  in cortex,  $^*P < 0.05$  vs sham  $^\#P < 0.05$  vs 2VO.) Abbreviations: Total, total dendrite; Pri, primary dendrite; Sec, secondary dendrite; Ter, tertiary dendrite. I: Representative TUNEL photomicrographs in hippocampal CA1 and DG and cortex of 2VO rats with or without lenti-pre-*miR-195* treatment at 20 $\times$  magnification. J: Representative Nissl staining photomicrographs in hippocampal CA1 and DG and cortex of 2VO rats with or without lenti-pre-*miR-195* treatment at 20 $\times$  magnification.



**Fig. 19 Schematic diagram of *miR-195* mediated A $\beta$  aggregation, tau hyperphosphorylation, dendritic degeneration and neuron death in CBH**

First, CBH elicits the elevation of NF- $\kappa$ B, which binds with the promoter sequence of *miR-195* and negatively regulates the expression of *miR-195*. Second, down-regulated *miR-195* induces the up-regulation of APP and BACE1 and leads to an increase in A $\beta$  levels. Third, some of the elevated A $\beta$  then enter the intracellular space and activate calpain, which promotes the conversion of CDK5/p35 to CDK5/p25 and catalyzes the degradation of I $\kappa$ B; I $\kappa$ B is an inhibitor of NF- $\kappa$ B, which activates NF- $\kappa$ B. CDK5/p25 directly phosphorylates tau. Fourth, down-regulated *miR-195* induces an up-regulation of p35, which provides the active substrates of p25. Fifth, A $\beta$  aggregation inactivates PP2A by inhibiting the expression of LCMT-1 and promotes the conversion of CDK5/p35 to CDK5/p25 to phosphorylating tau. In addition, down-regulation of *miR-195* direct up-regulates PME-1 expression, which inactive PP2A by inhibits methylation level of PP2A $\alpha$  at Leu309 residue. Sixth, decreased activation of PP2A also activates NF- $\kappa$ B, which in turn inhibits the expression of *miR-195*. Seventh, down-regulated *miR-195* could promote N-APP expression through cleaving of APP by BACE1 and posttranscriptionally up-regulate DR6. Over-produced N-APP binding with up-regulated DR6 results dendritic remodeling and neuron death through activating caspase 3 and caspase 6.

CBH: chronic brain hypoperfusion ; NF- $\kappa$ B: nuclear factor- $\kappa$ B; APP: amyloid precursor protein; BACE1:  $\beta$ -site APP cleaving enzyme 1; CDK5/p35: cyclin-dependent kinase 5; PP2A: protein phosphatase-2A ; LCMT-1: leucine carboxyl methyltransferase-1; PME-1: methylesterase; N-APP: N-terminal  $\beta$ -amyloid precursor protein; DR6: death receptor-6.

由于 miRNAs 作用的复杂性,相信会有更多的 miRNAs 参与 CBH 条件下的不同的病理生理过程。阐明 CBH 诱导痴呆发生的分子机制仍然任重道远。

## 参 考 文 献

- [1] Annemieke Ruitenberg, Tom den Heijer, Stef L M Bakker, et al. Cerebral hypoperfusion and clinical onset of dementia: the Rotterdam Study [J]. Ann Neurol, 2005, 57(6): 789-794.
- [2] Mak Adam Daulatzai. Cerebral hypoperfusion and glucose hypometabolism: key pathophysiological modulators promote neurodegeneration, cognitive impairment, and Alzheimer's disease [J]. J Neurosci Res, 2017, 95(4): 943-972.
- [3] Eszter Farkas, Paul G M Luiten, Ferenc Bari. Permanent, bilateral common carotid artery occlusion in the rat: a model for chronic cerebral hypoperfusion-related neurodegenerative diseases [J]. Brain Res Rev, 2007, 54(1): 162-180.
- [4] Seth Love, J Scott Miners. Cerebrovascular disease in ageing and Alzheimer's disease [J]. Acta Neuropathol, 2016, 131(5): 645-658.
- [5] Cai Zhi-you, Yan Yong, Sun Shanquan, et al.

- Upregulation of BACE1 and beta-amyloid protein mediated by chronic cerebral hypoperfusion contributes to cognitive impairment and pathogenesis of Alzheimer's disease [J]. *Neurochem Res*, 2009, 34(7): 1226-1235.
- [6] Vincent Boissonneault, Isabelle Plante, Serge Rivest, et al. *MicroRNA-298 and microRNA-328 regulate expression of mouse beta-amyloid precursor protein-converting enzyme 1* [J]. *J Biol Chem*, 2009, 284(4): 1971-1981.
- [7] Quinlan S, Kenny A, Medina M, et al. MicroRNAs in neurodegenerative diseases [J]. *Int Rev Cell Mol Biol*, 2017, 334: 309-343.
- [8] Sebastien S Hebert, Katrien Horre, Laura Nicolai, et al. Loss of microRNA cluster miR-29a/b-1 in sporadic Alzheimer's disease correlates with increased BACE1/beta-secretase expression [J]. *Proc Natl Acad Sci USA*, 2008, 105(17): 6415-6420.
- [9] Zong Yuan-yuan, Wang Hai-lin, Dong Wei, et al. miR-29c regulates BACE1 protein expression [J]. *Brain Res*, 2011, 1395: 108-115.
- [10] 车慧, 杨宝峰, 艾静. MicroRNA 在学习记忆功能障碍中的作用 [J]. 神经药理学报. 2011, 1(4): 26-32.
- [11] Kristin T Jacobsen, Kerstin Iverfeldt. Amyloid precursor protein and its homologues: a family of proteolysis-dependent receptors [J]. *Cell Mol Life Sci*, 2009, 66(14): 2299-2318.
- [12] Jing Ai, Li-Hua Sun, Hui Che, et al. *MicroRNA-195 protects against dementia induced by chronic brain hypoperfusion via its anti-amyloidogenic effect in rats* [J]. *J Neurosci*, 2013, 33(9): 3989-4001.
- [13] Piotr Lewczuk, Hermann Esselmann, Mirko Bibl, et al. Tau protein phosphorylated at threonine 181 in CSF as a neurochemical biomarker in Alzheimer's disease: original data and review of the literature [J]. *J Mol Neurosci*, 2004, 23(1-2): 115-122.
- [14] Gentry N Patrick, Lawrence Zukerberg, Margareta Nikolic, et al. Conversion of p35 to p25 deregulates Cdk5 activity and promotes neurodegeneration [J]. *Nature*, 1999, 402(6762): 615-622.
- [15] Sun Li-hua, Ban Tao, Liu Cheng-di, et al. Activation of Cdk5/p25 and tau phosphorylation following chronic brain hypoperfusion in rats involves *microRNA-195* downregulation [J]. *J Neuro chem*, 2015, 134(6): 1139-1151.
- [16] Ludovic Martin, Xenia Latypova, Cornelia M Wilson, et al. Tau protein phosphatases in Alzheimer's disease: the leading role of PP2A [J]. *Ageing Res Rev*, 2013a, 12(1): 39-49.
- [17] Ludovic Martin, Xenia Latypova, Cornelia M Wilson, et al. Tau protein kinases: involvement in Alzheimer's disease [J]. *Ageing Res Rev*, 2013b, 12(1): 289-309.
- [18] Ward Sents, Elitsa Ivanova, Caroline Lambrecht, et al. The biogenesis of active protein phosphatase 2A holoenzymes: a tightly regulated process creating phosphatase specificity [J]. *FEBS J*, 2013, 280(2): 644-661.
- [19] Joana Oliveira, Marcio Costa, Maria Soares Cachide de Almeida, et al. Protein phosphorylation is a key mechanism in Alzheimer's disease [J]. *J Alzheimers Dis*, 2017, 58(4): 953-978.
- [20] Xing Yong-na, Li Zhu, Chen Yu, et al. Structural mechanism of demethylation and inactivation of protein phosphatase 2A [J]. *Cell*, 2008, 133(1): 154-163.
- [21] Yao Xiu-qing, Zhang Xiao-xue, Yin Yang-yang, et al. Glycogen synthase kinase-3beta regulates Tyr307 phosphorylation of protein phosphatase-2A via protein tyrosine phosphatase 1B but not Src [J]. *Biochem J*, 2011, 437(2): 335-344.
- [22] Li Mei, Damuni Zahi. I1PP2A and I2PP2A. Two potent protein phosphatase 2A-specific inhibitor proteins [J]. *Methods Mol Biol*, 1998, 93: 59-66.
- [23] Liu Cheng-di, Wang Qin, Zong De-kang, et al. Knockdown of *microRNA-195* contributes to protein phosphatase-2A inactivation in rats with chronic brain hypoperfusion [J]. *Neurobiol Aging*, 2016, 45: 76-87.
- [24] Natalia Salvadores, Mario Sanhueza, Patricio Manque, et al. Axonal degeneration during aging and its functional role in neurodegenerative disorders [J]. *Front Neurosci*, 2017, 11:451.
- [25] Wilson M Alobuia, Xia Wei, Bhupinder P S Vohra. Axon degeneration is key component of neuronal death in amyloid-beta toxicity [J]. *Neurochem Int*, 2013, 63(8): 782-789.
- [26] Anatoly Y Nikolaev, T G Von McLaughlin, Dennis D M O'Leary, et al. APP binds DR6 to trigger axon pruning and neuron death via distinct caspases [J]. *Nature*, 2009, 457(7232): 981-989.
- [27] Chen Xin, Jiang Xue-mei, Zhao Lin-jing, et al.

- MicroRNA-195 prevents dendritic degeneration and neuron death in rats following chronic brain hypoperfusion [ J ]. Cell Death Dis, 2017, 8(6):e2850.
- [ 28 ] Sangyun Jeong. Molecular and cellular basis of neurodegeneration in Alzheimer's disease [ J ]. Mol Cells, 2017, 40(9): 613-620.
- [ 29 ] Marta Crous-Bou, Carolina Minguillón, Nina Gramunt, et al. Alzheimer's disease prevention: from risk factors to early intervention [ J ]. Alzheimers Res Ther, 2017, 9(1):71.